Inorganic Scintillators for Future Crystal Calorimeters

Ren-Yuan Zhu

California Institute of Technology

March 16, 2021

Why Crystal Calorimetry?

- Precision photons and electrons measurements enhance physics discovery potential in HEP experiments.
- Performance of crystal calorimeters is well understood for e/γ, and is promising for jets measurements :
  - The best possible energy resolution and position resolution;
  - Good e/γ identification and reconstruction efficiency;
  - Excellent jet mass resolution with dual readout, either C/S and F/S gate.
- The next generation crystal calorimeters for HEP:
  - Ultra-compact, rad-hard LYSO/LuAG ceramics RADiCAL for HL-LHC/FCC-hh;
  - Ultrafast BaF_2:Y calorimetry to face the challenge of unprecedented rate;
  - Longitudinally segmented crystal calorimeter for the Higgs factory: Calvision and homogeneous hadron calorimeter (HHCAL).

Existing Crystal Calorimeters in HEP

Date	75-85	80-00	80-00	80-00	90-10	94-10	94-10	95-Now	10-Now
Experiment	C. Ball	L3	CLEO II	C. Barrel	KTeV	BaBar	BELLE	CMS	BES III
Accelerator	SPEAR	LEP	CESR	LEAR	Tevatron	PEP	KEKB	LHC	BEPC
Laboratory	SLAC	CERN	Cornell	CERN	FNAL	SLAC	KEK	CERN	IHEP
Crystal Type	NaI:Tl	BGO	CsI:Tl	CsI:Tl	CsI	CsI:Tl	CsI:Tl	PWO	CsI:Tl
B-Field（T）	-	0.5	1.5	1.5	-	1.5	1.0	4.0	1.0
r_{inner} (m)	0.254	0.55	1.0	0.27	-	1.0	1.25	1.29	0.94
Crystal number	672	11,400	7,800	1,400	3,300	6,580	8,800	75,848	6,240
Crystal Depth（X_0）	16	22	16	16	27	16 to 17.5	16.2	25	15
Crystal Volume（m^3）	1	1.5	7	1	2	5.9	9.5	11	5.3
Light Output（p.e./MeV）	350	1,400	5,000	2,000	40	5,000	5,000	2	5,000
Photo-detector	PMT	Si PD	Si PD	WS+Si PD	PMT	Si PD	Si PD	Si APD	Si PD
Gain of Photo-detector	Large	1	1	1	4,000	1	1	50	1
σ_N/Channel（MeV）	0.05	0.8	0.5	0.2	Small	0.15	0.2	40	0.2
Dynamic Range	10^4	10^5	10^4	10^4	10^4	10^4	10^4	10^5	10^4

Crystals with Mass Production Capability

Crystal	NaI:Tl	CsI:Tl	CsI	BaF_2	CeF_3	PbF_2	BGO	BSO	$PbWO_4$	LYSO:Ce	AFO Glasses	Sapphire:Ti
Density (g/cm^3)	3.67	4.51	4.51	4.89	6.16	7.77	7.13	6.8	8.3	7.40	4.6	3.98
Melting points (^{o}C)	651	621	621	1280	1460	824	1050	1030	1123	2050	-	2040
X_0 (cm)	2.59	1.86	1.86	2.03	1.65	0.94	1.12	1.15	0.89	1.14	2.96	7.02
R_M (cm)	4.13	3.57	3.57	3.10	2.39	2.18	2.23	2.33	2.00	2.07	2.89	2.88
λ_I (cm)	42.9	39.3	39.3	30.7	23.2	22.4	22.7	23.4	20.7	20.9	26.4	24.2
Z_{eff}	50.1	54.0	54.0	51.6	51.7	77.4	72.9	75.3	74.5	64.8	42.8	11.2
dE/dX (MeV/cm)	4.79	5.56	5.56	6.52	8.40	9.42	8.99	8.59	10.1	9.55	6.84	6.75
λ_{peak} ^{a} (nm)	410	560	420 310	300 220	340 300	\	480	470	425 420	420	365	300 750
Refractive Index^b	1.85	1.79	1.95	1.50	1.62	1.82	2.15	2.68	2.20	1.82	-	1.76
Normalized Light Yield^{a,c}	120	190	4.2 1.3	42 4.8	8.6	\	25	5	0.4 0.1	100	1.5	0.04 0.22
Total Light yield (ph/MeV)	35,000	58,000	1700	13,000	2,600	\	7,400	1,500	130	30,000	450	7,900
Decay time^a (ns)	245	1220	30 6	600 0.5	30	\	300	100	30 10	40	40	300 3200
Hygroscopic	Yes	Slight	Slight	No	No	No	No	No	No	No	No	No
Experiment	Crystal Ball	CLEO BaBar BELLE BES III	KTeV Mu2e	TAPS Mu2e-II?	-	A4 g-2	L3 BELLE	-	CMS ALICE PrimEx Panda	CMS BTL COMET HERD	HHCAL?	HHCAL?

Issue of PWO: Radiation Damage

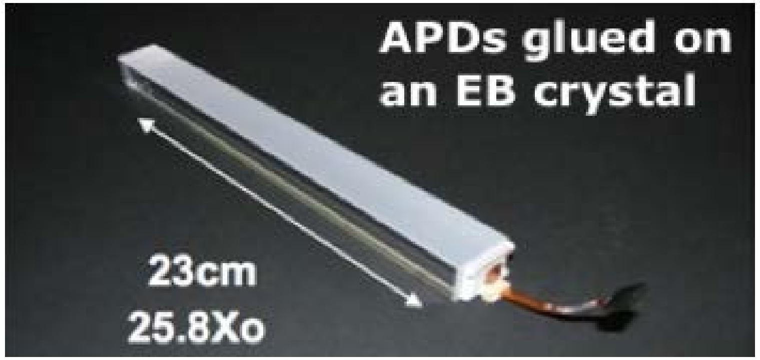

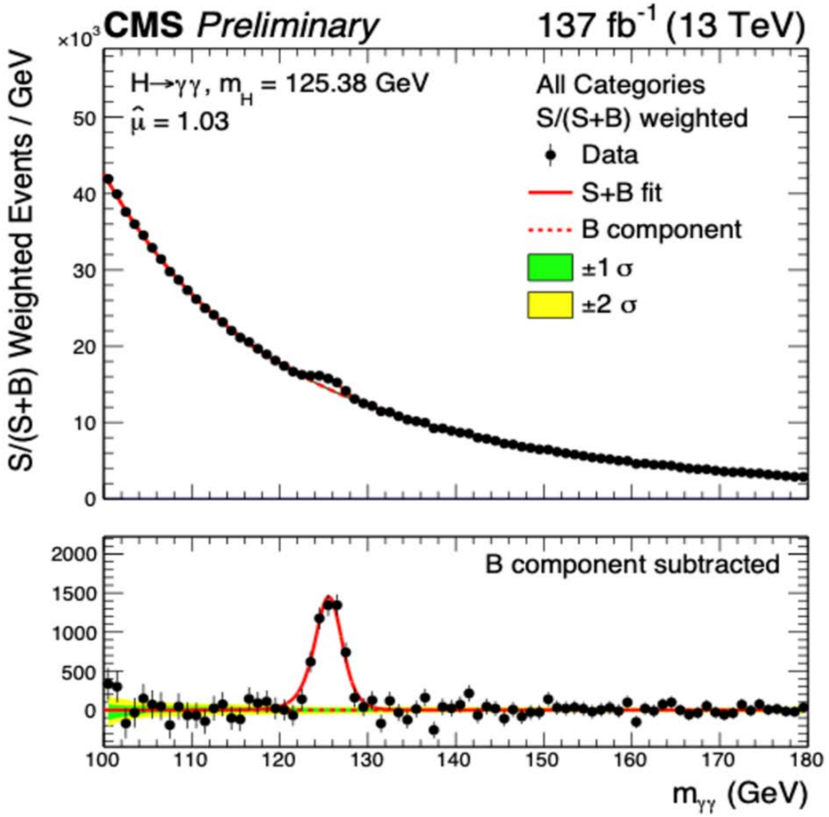

E. Auffray, in SINT 2019, Sep 2019

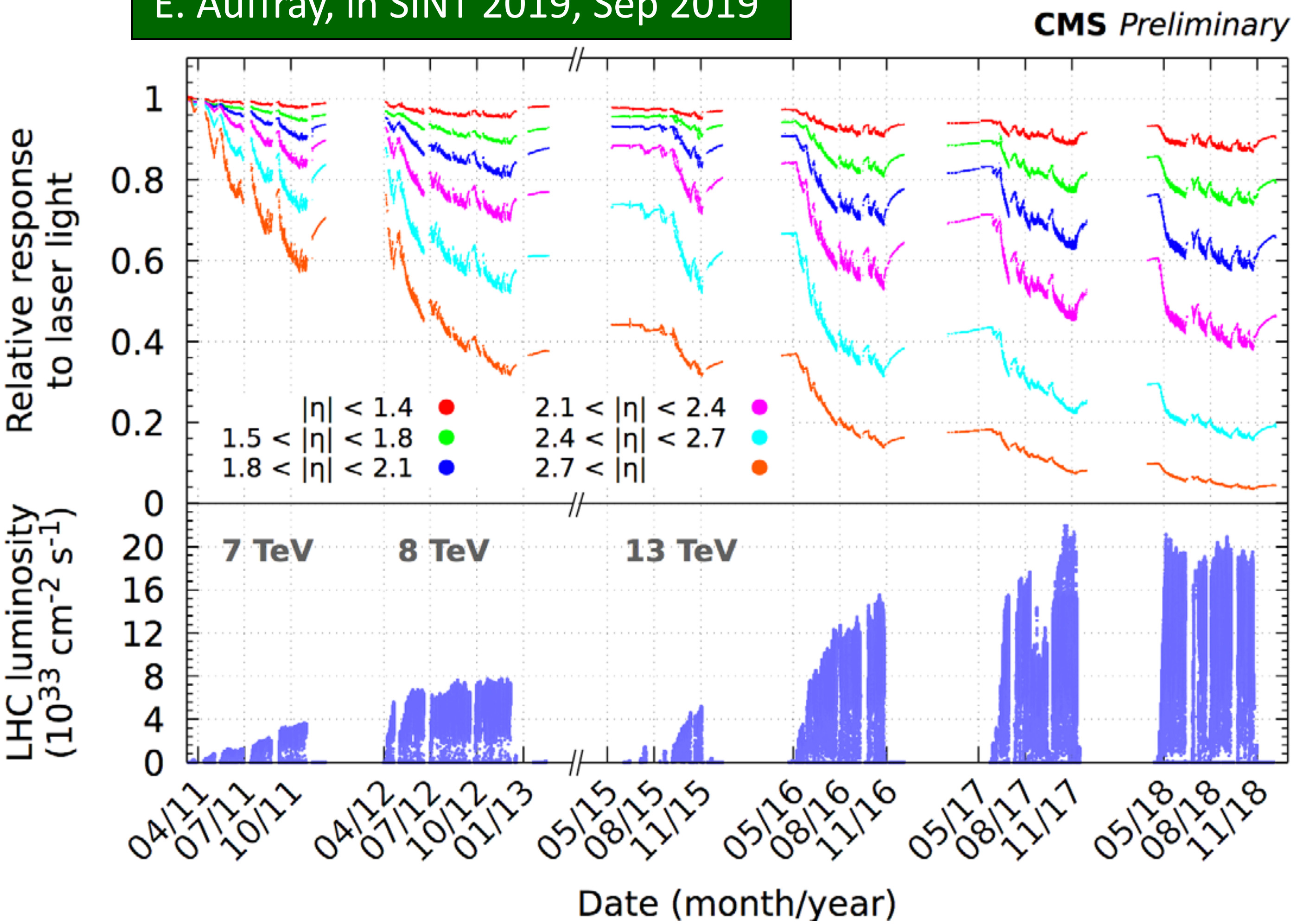

Excellent energy resolution by PWO+APD for Higgs discovery
The main issue of CMS ECAL: radiation damage in PWO crystals
Continuous monitoring are crucial to maintaining crystal precision

Dose Rate Dependent Damage in PWO

PWO light reached an equilibrium under a dose rate, showing a dose rate dependent damage. Monitoring data support damage by ɣ/p/n.

IEEE Trans. Nucl. Sci., Vol. 44 (1997) 458-476

Talk in CMS ECAL Days (2016)

$$dD = \sum_{i=1}^{n}\{-a_i D_i dt + (D_i^{all} - D_i)\, b_i R dt\}$$

$$D = \sum_{i=1}^{n}\{\frac{b_i R D_i^{all}}{a_i + b_i R}[1 - e^{-(a_i+b_iR)t}] + D_i^0 e^{-(a_i+b_iR)t}\}$$

- D_i: color center density in units of m^{-1};
- D_i^0: initial color center density;
- D_i^{all} is the total density of trap related to the color center in the crystal;
- a_i: recovery costant in units of hr^{-1};
- b_i: damage contant in units of kRad^{-1};
- R: the radiation dose rate in units of kRad/hr.

$$D_{eq} = \sum_{i=1}^{n}\frac{b_i R D_i^{all}}{a_i + b_i R}$$

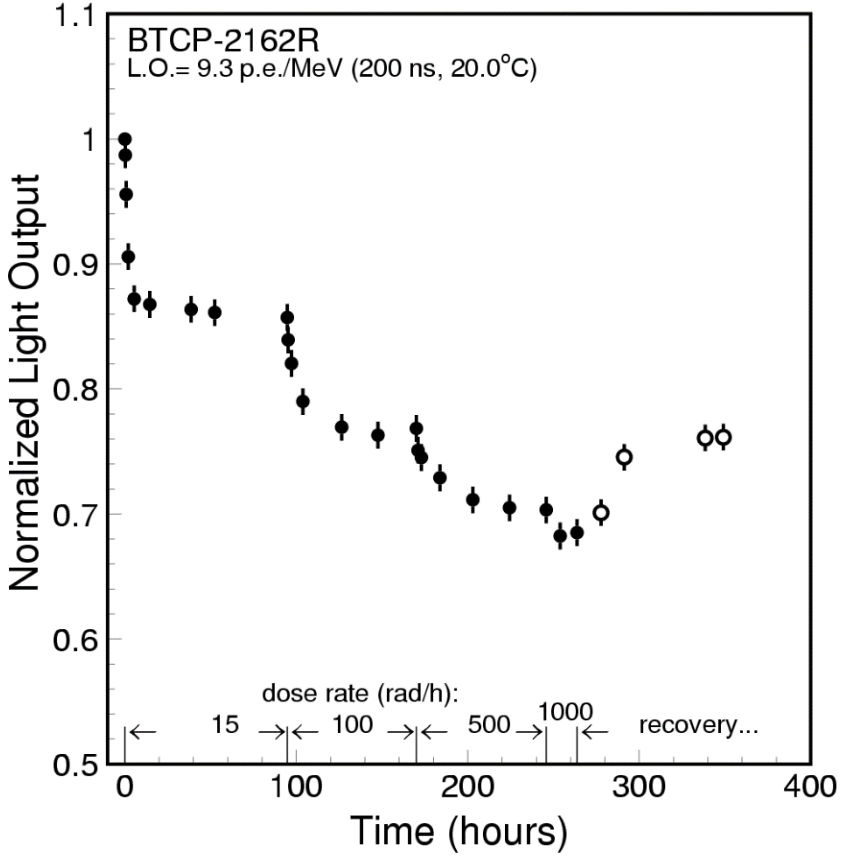

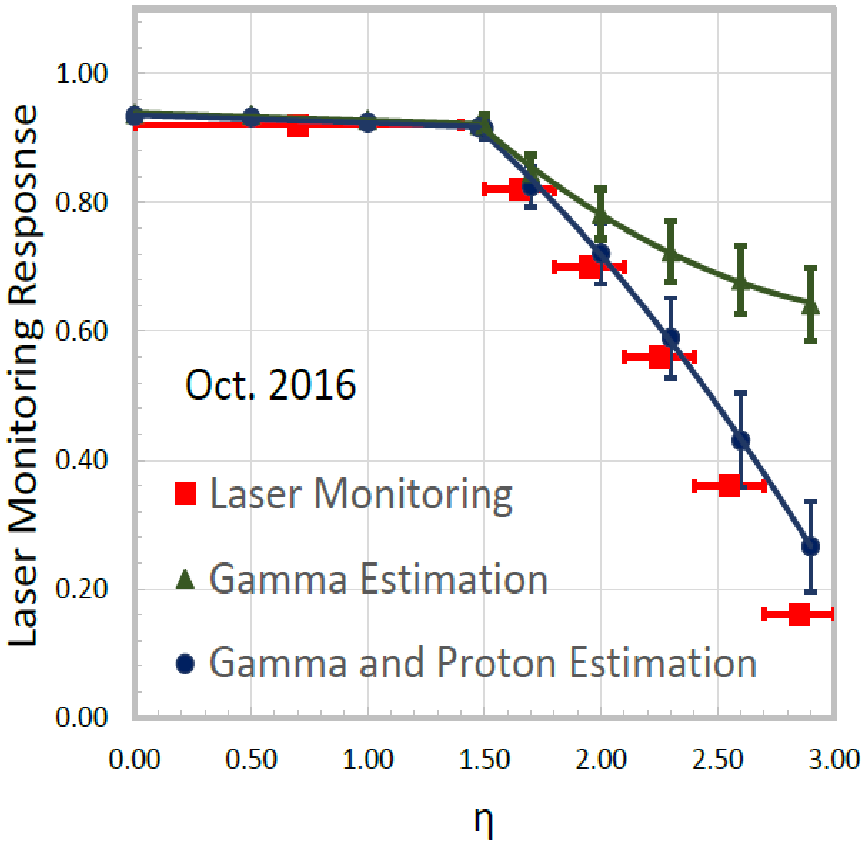

Oxygen Vacancies Identified by TEM/EDS

NIM A413 (1998) 297

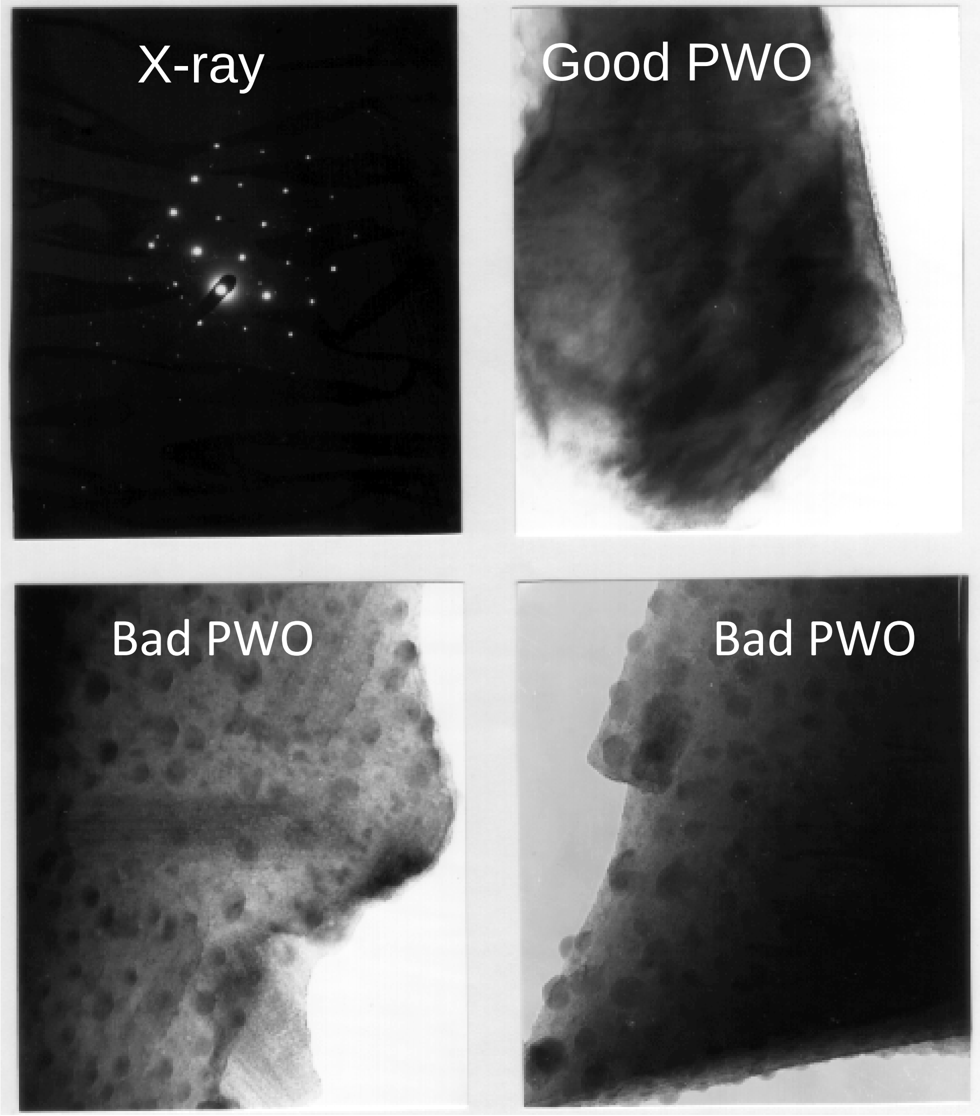

Atomic Fraction (%) in $PbWO_4$

As Grown Sample

Element	Black Spot	Peripheral	$Matrix_1$	$Matrix_2$
O	1.5	15.8	60.8	63.2
W	50.8	44.3	19.6	18.4
Pb	47.7	39.9	19.6	18.4

The Same Sample after Oxygen Compensation

Element	$Point_1$	$Point_2$	$Point_3$	$Point_4$
O	59.0	66.4	57.4	66.7
W	21.0	16.5	21.3	16.8
Pb	20.0	17.1	21.3	16.5

5 to10 nm black spots identified by TOPCON-002B TEM scope, 200 kV, 10 uA.

Localized stoichiometry analysis by JEOL JEM-2010 scope and Link ISIS EDS

2019 DOE Basic Research Needs Study on Instrumentation: Calorimetry

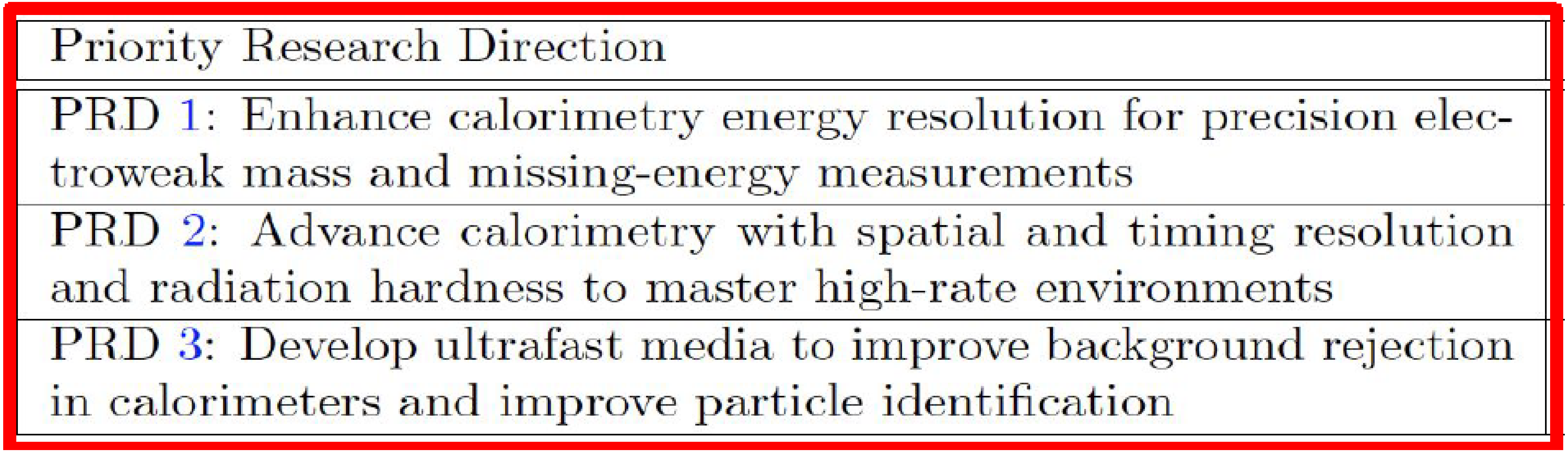

Priority Research Direction
PRD 1: Enhance calorimetry energy resolution for precision electroweak mass and missing-energy measurements
PRD 2: Advance calorimetry with spatial and timing resolution and radiation hardness to master high-rate environments
PRD 3: Develop ultrafast media to improve background rejection in calorimeters and improve particle identification

Energy, spatial and timing resolution, radiation hard and ultrafast calorimetry
Calorimetry session in 2021 CPAD HEP Instrumentation Frontier Workshop
https://indico.fnal.gov/event/46746/timetable/#all.detailed

Fast and Ultrafast Inorganic Scintillators

	BaF_2	BaF_2:Y	ZnO:Ga	YAP:Yb	YAG:Yb	β-Ga_2O_3	LYSO:Ce	LuAG:Ce	YAP:Ce	GAGG:Ce	LuYAP:Ce	YSO:Ce
Density (g/cm^3)	4.89	4.89	5.67	5.35	4.56	5.94[1]	7.4	6.76	5.35	6.5	7.2[f]	4.44
Melting points (°C)	1280	1280	1975	1870	1940	1725	2050	2060	1870	1850	1930	2070
X_0 (cm)	2.03	2.03	2.51	2.77	3.53	2.51	1.14	1.45	2.77	1.63	1.37	3.10
R_M (cm)	3.1	3.1	2.28	2.4	2.76	2.20	2.07	2.15	2.4	2.20	2.01	2.93
λ_I (cm)	30.7	30.7	22.2	22.4	25.2	20.9	20.9	20.6	22.4	21.5	19.5	27.8
Z_{eff}	51.6	51.6	27.7	31.9	30	28.1	64.8	60.3	31.9	51.8	58.6	33.3
dE/dX (MeV/cm)	6.52	6.52	8.42	8.05	7.01	8.82	9.55	9.22	8.05	8.96	9.82	6.57
λ_{peak}[a] (nm)	300 220	300 220	380	350	350	380	420	520	370	540	385	420
Refractive Index[b]	1.50	1.50	2.1	1.96	1.87	1.97	1.82	1.84	1.96	1.92	1.94	1.78
Normalized Light Yield[a,c]	42 4.8	1.7 4.8	6.6[d]	0.19[d]	0.36[d]	6.5 0.5	100	35[e] 48[e]	9 32	115	16 15	80
Total Light yield (ph/MeV)	13,000	2,000	2,000[d]	57[d]	110[d]	2,100	30,000	25,000[e]	12,000	34,400	10,000	24,000
Decay time[a] (ns)	600 0.5	600 0.5	<1	1.5	4	148 6	40	820 50	191 25	800 80	1485 36	75
LY in 1st ns (photons/MeV)	1200	1200	610[d]	28[d]	24[d]	43	740	240	391	640	125	318
40 keV Att. Leng. (1/e, mm)	0.106	0.106	0.407	0.314	0.439	0.394	0.185	0.251	0.314	0.319	0.214	0.334

The CMS MIP Timing Detector

MTD performance goal: 30-40 ps at the start degrading to < 60 ps at 3000 fb^{-1}

Barrel Timing Layer: arrays of LYSO crystal bars connected to SiPMs at both ends and readout by TOFHIR

Endcap Timing Layer: LGAD sensors readout by ETROC

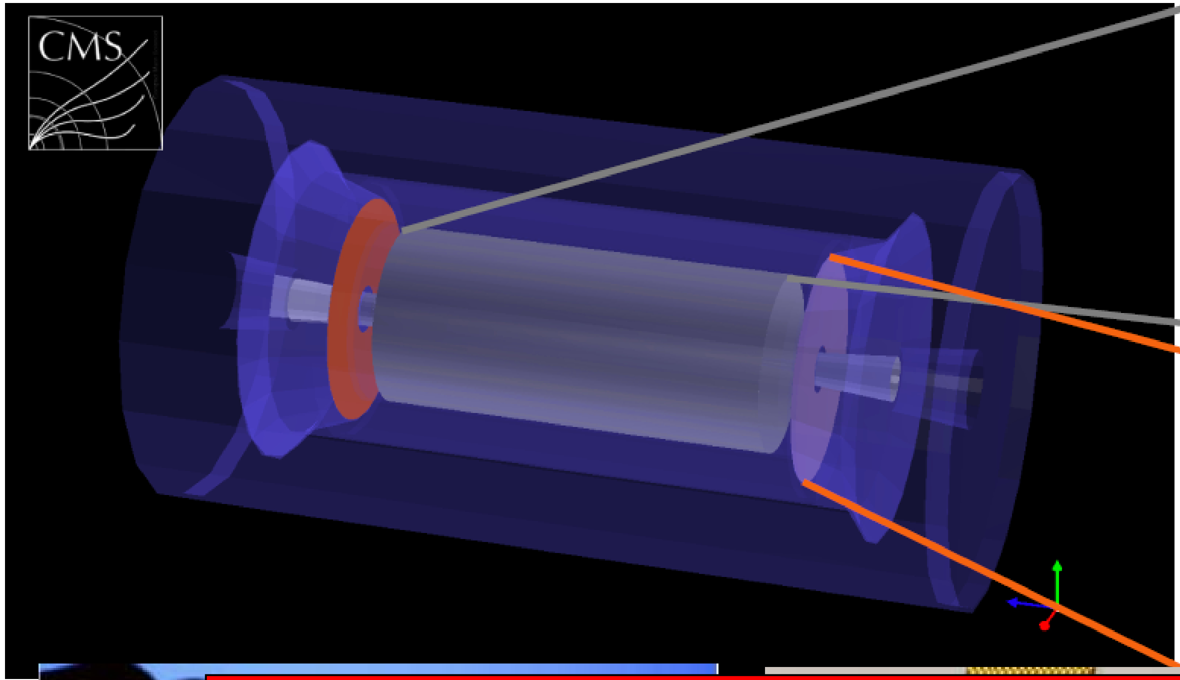

BTL: LYSO bars + SiPM read-out

- ▻ TK / ECAL interface ~ 45 mm thick
- ▻ $|\eta| < 1.45$ and $p_T > 0.7$ GeV
- ▻ Active area ~ 38 m^2 ; 332k channels
- ▻ Fluence at 3 ab^{-1}: 2×10^{14} n_{eq}/cm^2

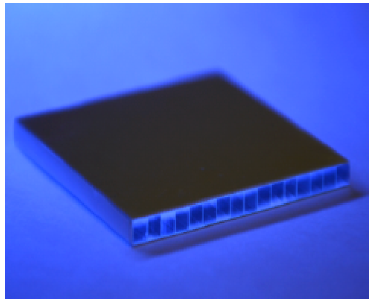

ETL: Si with internal gain (LGAD)

- ▻ On the HGC nose ~ 65 mm thick
- ▻ $1.6 < |\eta| < 3.0$
- ▻ Active area ~ 14 m^2; ~ 8.5M channels
- ▻ Fluence at 3 ab^{-1}: up to 2×10^{15} n_{eq}/cm^2

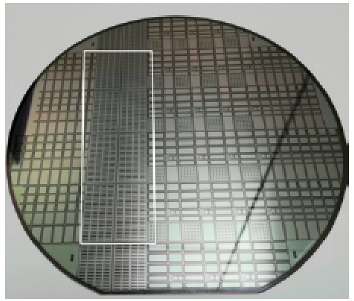

LYSO + SiPM with Thermal Electric Cooler (TEC) for CMS Barrel Timing Layer (BTL) in construction

1 x 16 LYSO:Ce bars

SiPM array prototypes from FBK

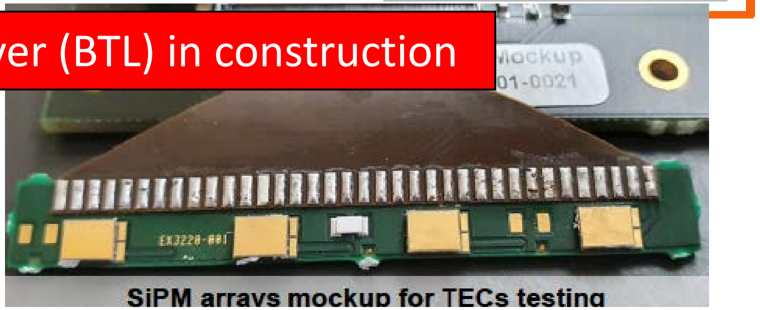

SiPM arrays mockup for TECs testing

CMS MTD: Expected Radiation

CMS MTD/FCAL: 4.8/68 Mrad, $2.5\times10^{13}/2.1\times10^{14}$ p/cm^2 & $3.2\times10^{14}/2.4\times10^{15}$ n_{eq}/cm^2

CMS MTD	η	n_{eq} (cm^{-2})	n_{eq} Flux (cm^{-2}s^{-1})	Protons (cm^{-2})	p Flux (cm^{-2}s^{-1})	Dose (Mrad)	Dose rate (rad/h)
Barrel	0.00	2.48E+14	2.75E+06	2.2E+13	2.4E+05	2.7	108
Barrel	1.15	2.70E+14	3.00E+06	2.4E+13	2.6E+05	3.8	150
Barrel	**1.45**	**2.85E+14**	**3.17E+06**	**2.5E+13**	**2.8E+05**	**4.8**	**192**
Endcap	1.60	2.3E+14	2.50E+06	2.0E+13	2.2E+05	2.9	114
Endcap	2.00	4.5E+14	5.00E+06	3.9E+13	4.4E+05	7.5	300
Endcap	2.50	1.1E+15	1.25E+07	9.9E+13	1.1E+06	25.5	1020
Endcap	**3.00**	**2.4E+15**	**2.67E+07**	**2.1E+14**	**2.3E+06**	**67.5**	**2700**

Much higher at FCC-hh: up to 0.1/500 Grad and $3\times10^{16}/5\times10^{18}$ n_{eq}/cm^2 at EMEC/EMF

M. Aleksa *et al.*, Calorimeters for the FCC-hh CERN-FCCPHYS-2019-0003, Dec 23, 2019

LYSO Radiation Hardness

CMS LYSO spec: RIAC < 3 m^{-1} after 4.8 Mrad, 2.5 x 10^{13} p/cm^2 and 3.2 x 10^{14} n_{eq}/cm^2

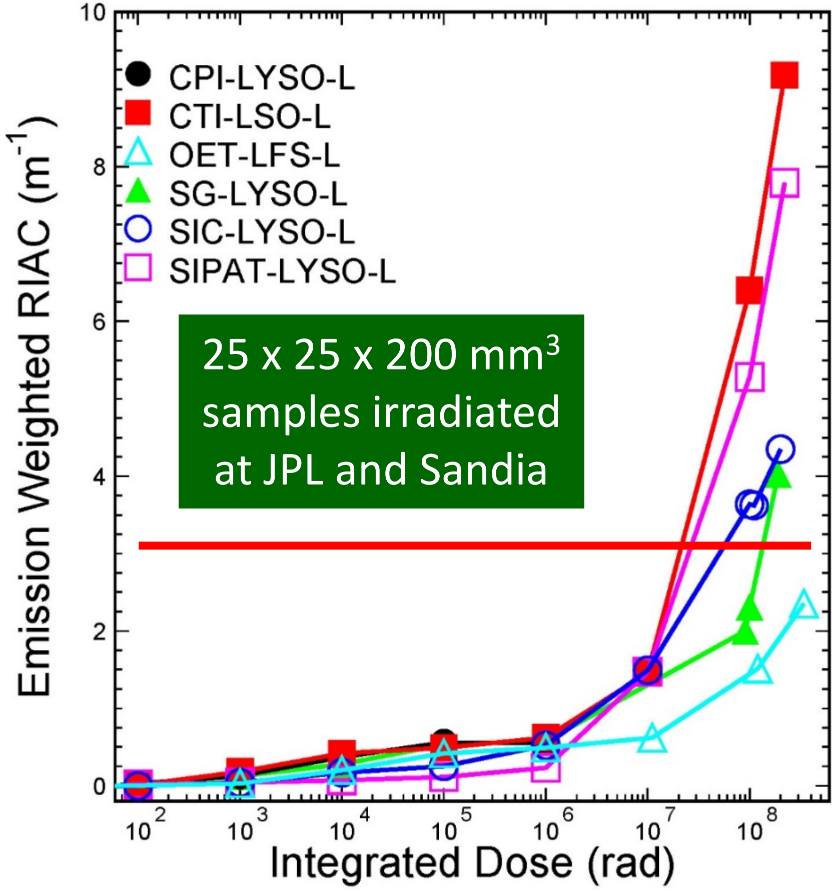

25 x 25 x 200 mm^3 samples irradiated at JPL and Sandia

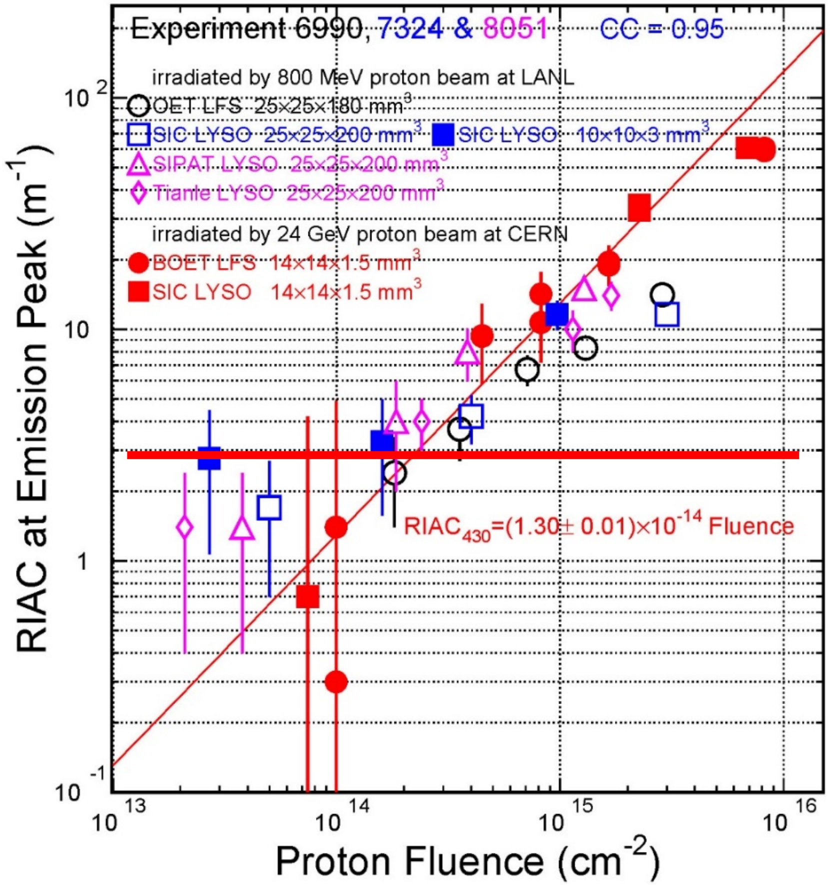

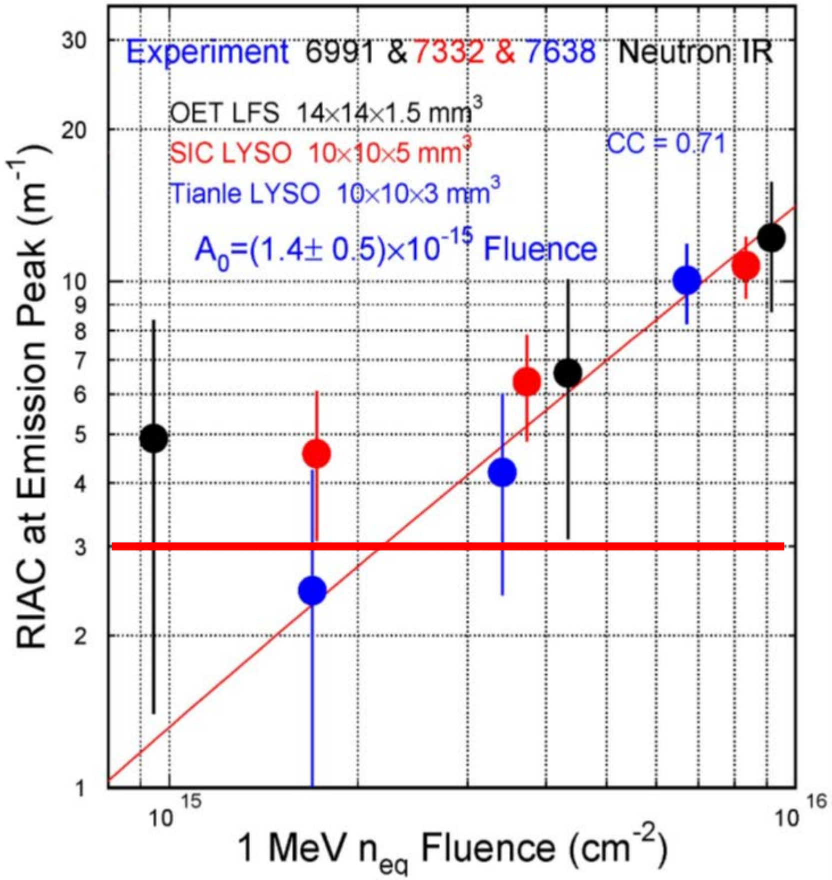

Damage induced by protons is an order of magnitude larger than that from neutrons
Due to ionization energy loss in addition to displacement and nuclear breakup

Radiation Hard LuAG:Ce Ceramics

LuAG:Ce ceramics shows a factor of two better radiation hardness than LYSO crystals up to 6.7$\times 10^{15}$ n_{eq}/cm^2 and 1.2$\times 10^{15}$ p/cm^2, promising for FCC-hh

Paper N18-05 in the virtual IEEE NSS/MIC 2020 Conference Record (2020)

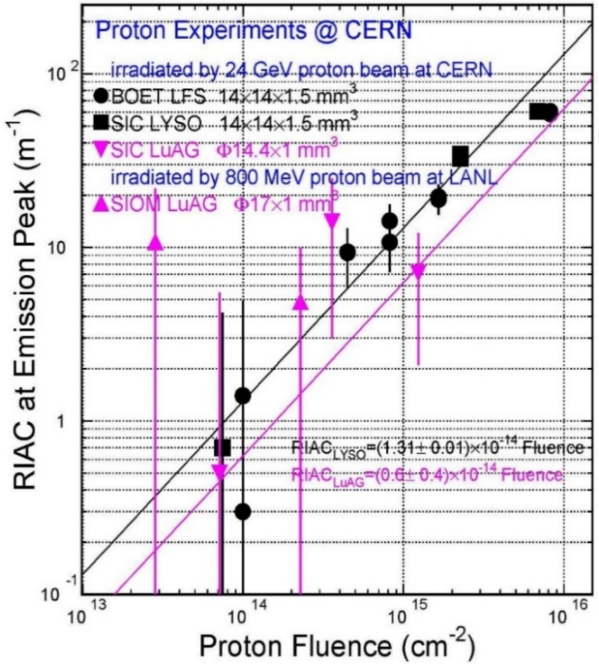

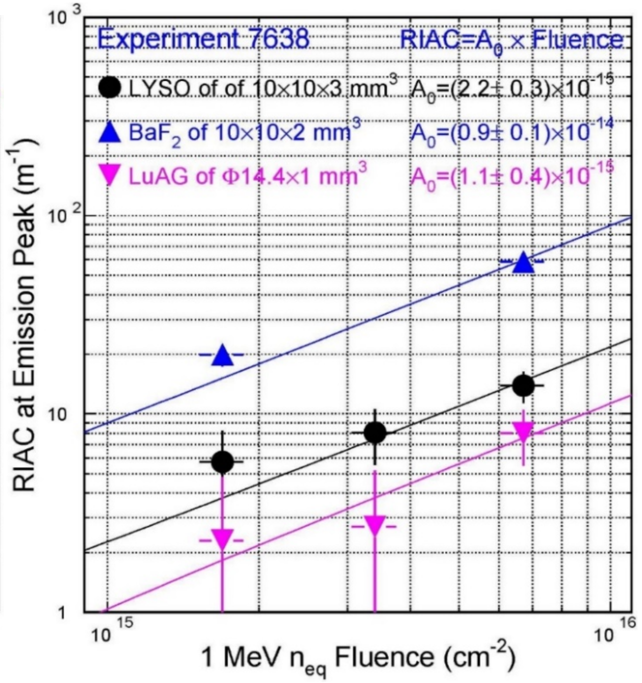

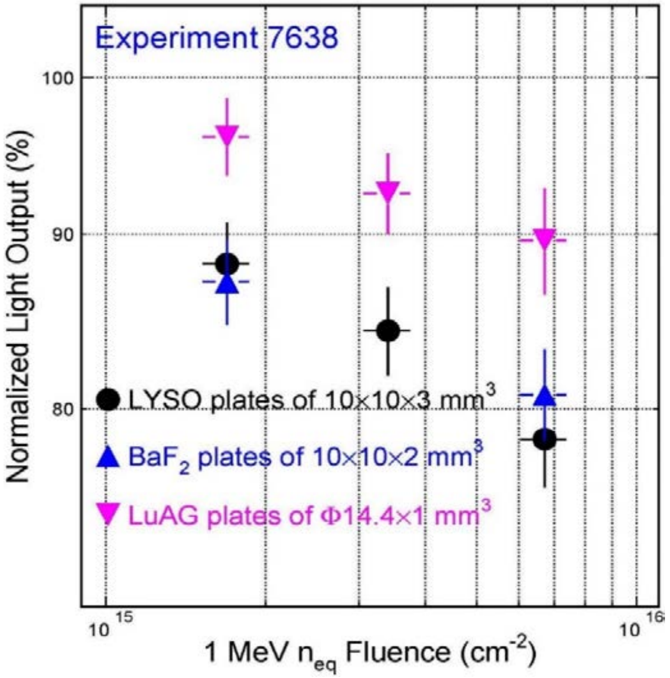

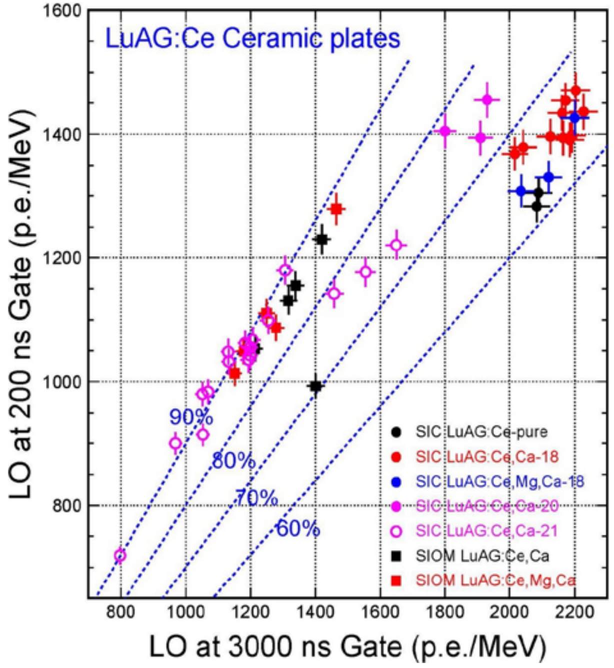

R&D on slow component suppression by e.g. Ca co-doping, and radiation hardness by ɣ/p/n

RADiCAL: LYSO/LuAG Shashlik CAL

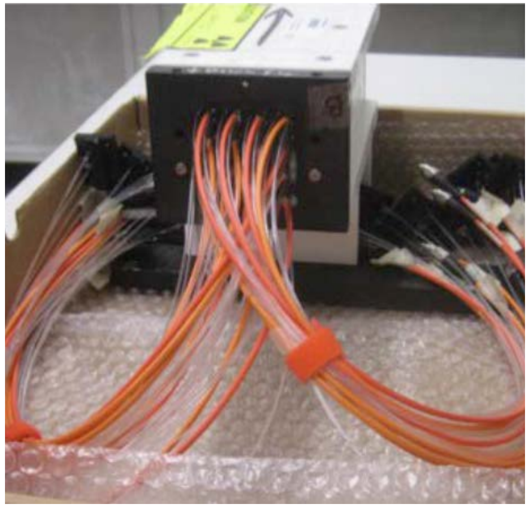

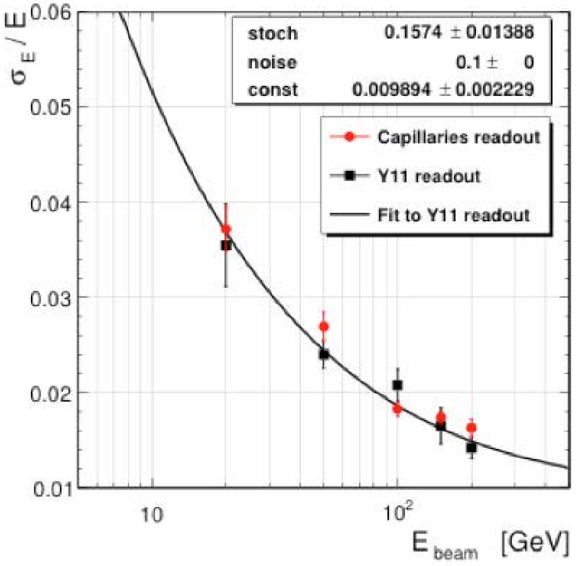

A 4x4 LYSO/DSB1 capillaries show consistent resolution with LYSO/Y11

Excitation of LuAG:Ce ceramics matches well LYSO:Ce emission: RADiCAL

RADiation hard **i**nnovative **CAL**orimetry

R. Ruchti, in the 2021 CPAD workshop

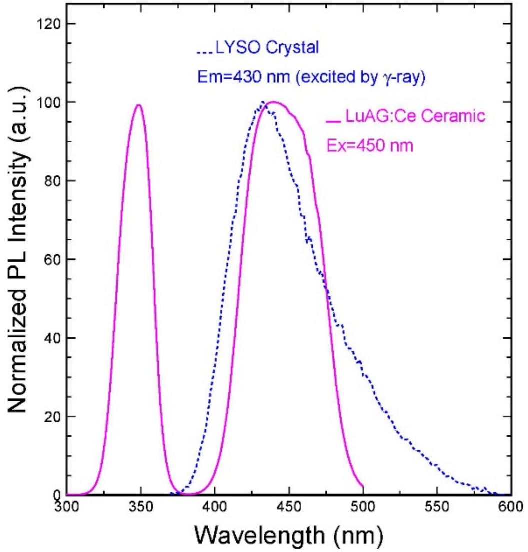

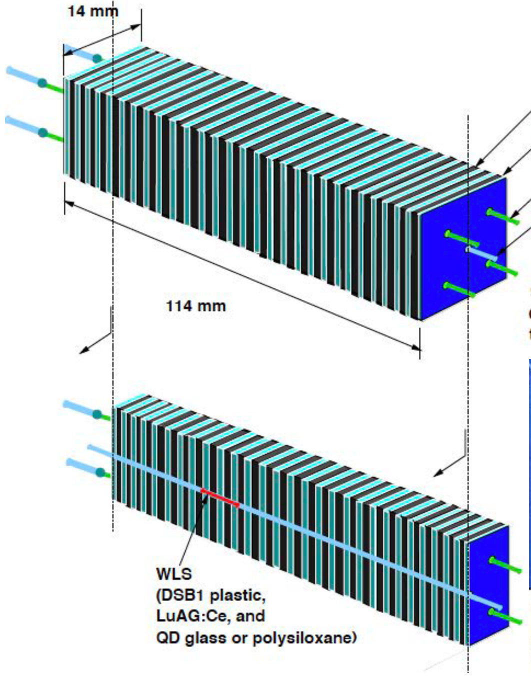

Φ1x40 mm SIC LuAG:Ce ceramic LHPG fibers

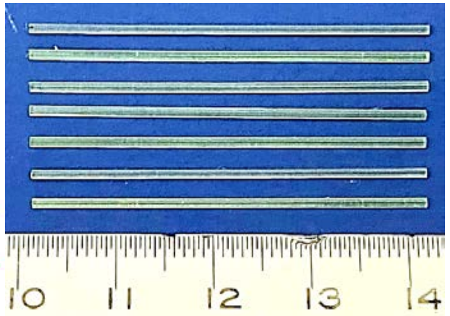

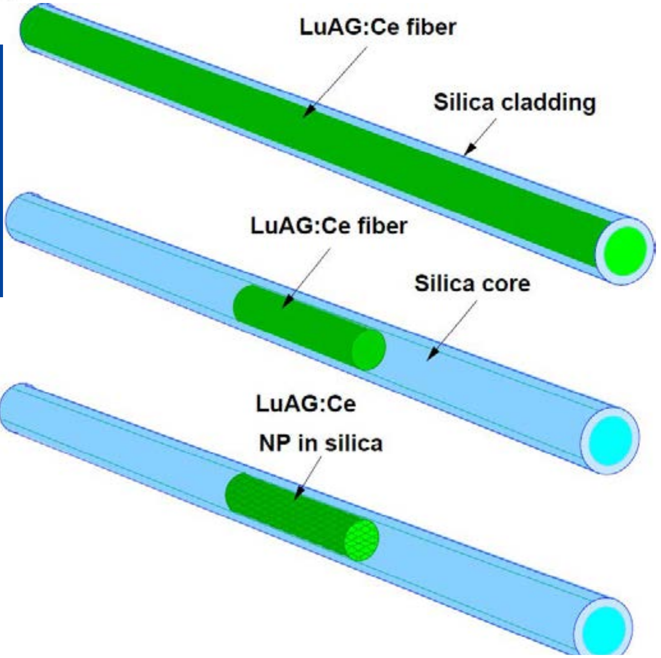

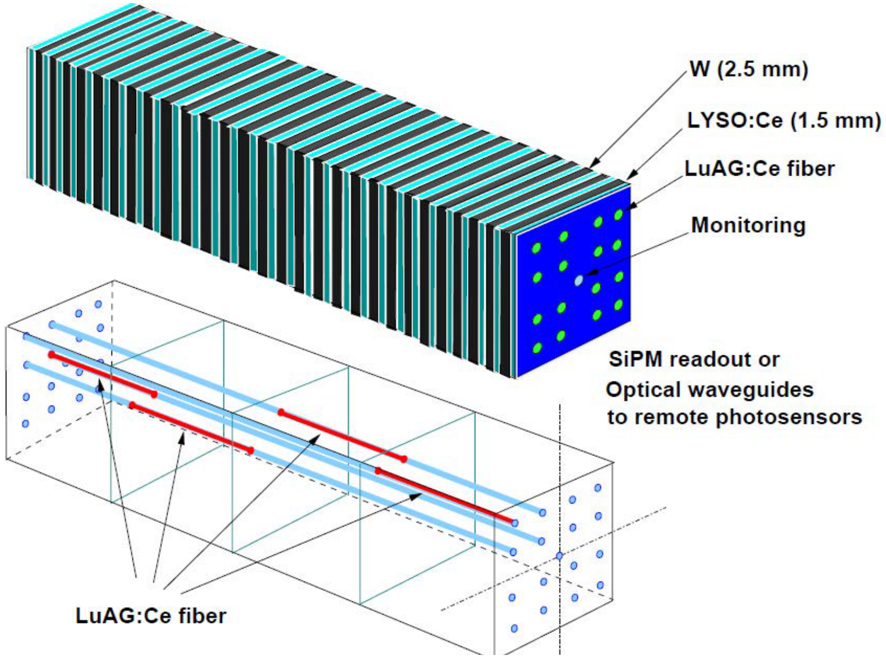

Mu2e Calorimeter Requirements

• Energy resolution	σ < 5% (FWHM/2.36) @ 100 MeV
• Time resolution	σ < 500 ps
• Position resolution	σ < 10 mm
• Radiation hardness • Crystals • Photosensors	 1 kGy/yr and a total of 10^{12} n_1 MeV equivalent/cm^2 total 3 x 10^{11} n_1 MeV equivalent/cm^2 total

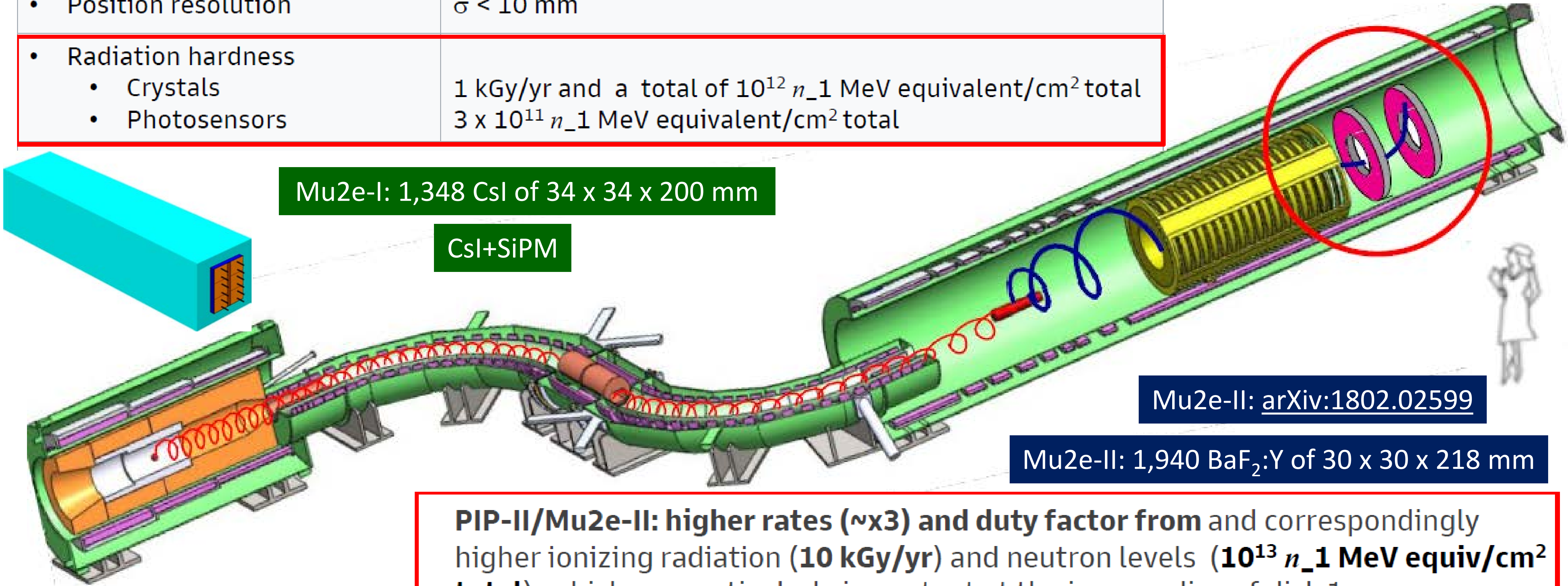

Mu2e-I: 1,348 CsI of 34 x 34 x 200 mm

CsI+SiPM

Mu2e-II: arXiv:1802.02599

Mu2e-II: 1,940 BaF$_2$:Y of 30 x 30 x 218 mm

PIP-II/Mu2e-II: higher rates (~x3) and duty factor from and correspondingly higher ionizing radiation (**10 kGy/yr**) and neutron levels (**10^{13} n_1 MeV equiv/cm^2 total**), which are particularly important at the inner radius of disk 1

Ultrafast and Slow Light from BaF$_2$

BaF$_2$ has a ultrafast scintillation component @ 220 nm with 0.5 ns decay time and an intensity similar to undoped CsI. It has also a factor of 5 larger slow component @ 300 nm with 300 ns decay time.

Slow suppression may be achieved by rare earth (Y, La and Ce) doping, and/or solar-blind photo-detectors, e.g. Cs-Te, K-Cs-Te and Rb-Te cathode

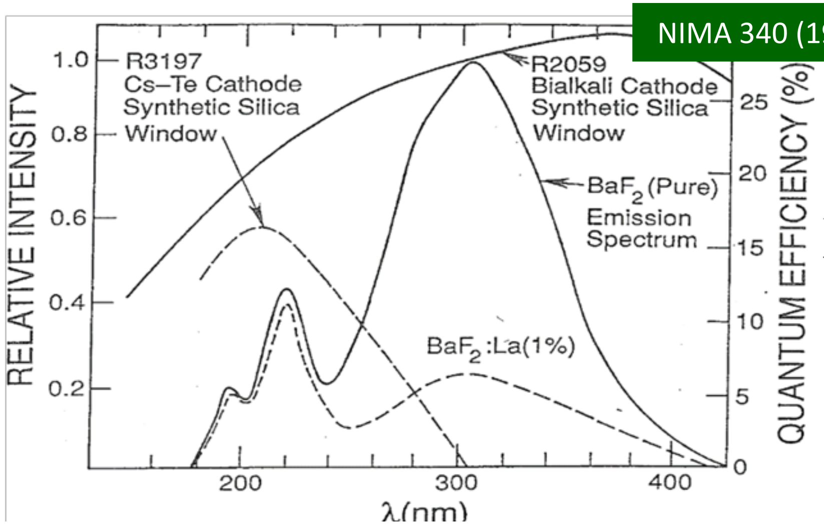

NIMA 340 (1994) 442-457

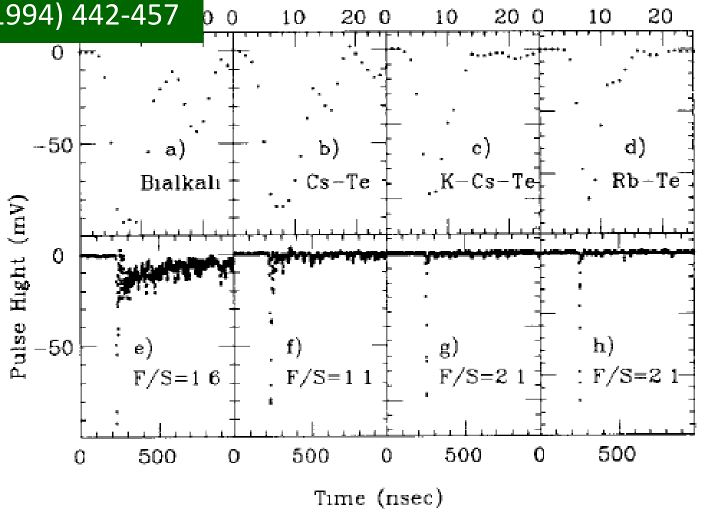

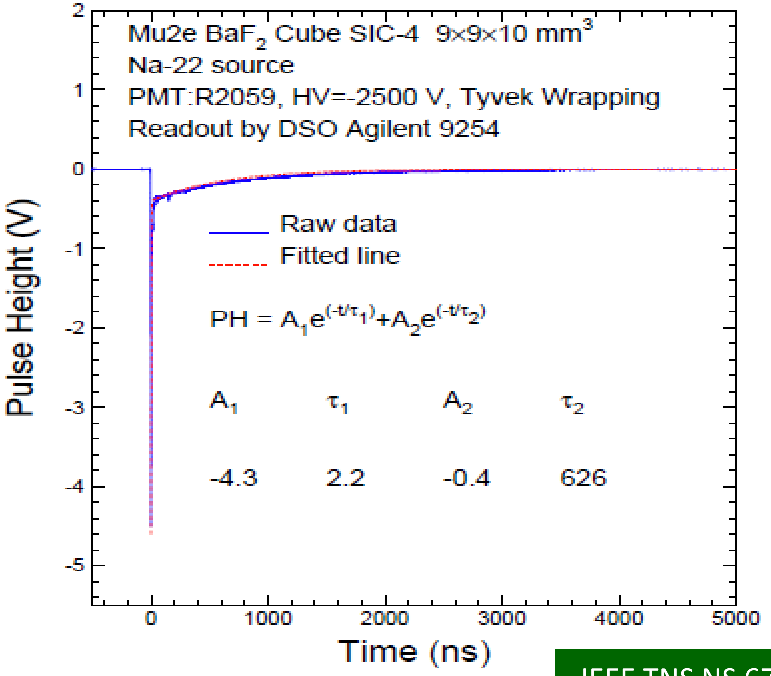

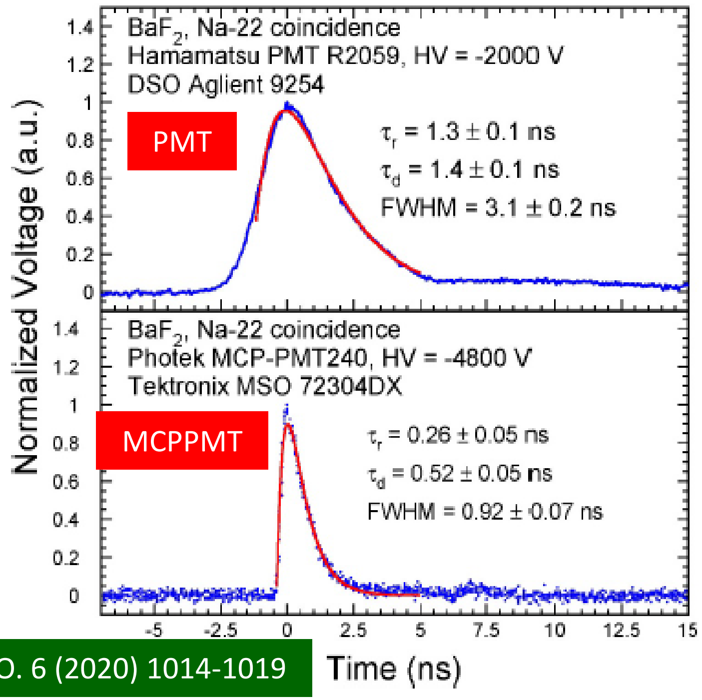

IEEE TNS NS 67, NO. 6 (2020) 1014-1019

γ-Ray Induced Damage in BaF_2

BaF_2 shows saturated damage from 10 krad to 100 Mrad, indicating good radiation resistance against ɣ-rays

IEEE TNS **63** (2016) 612-619

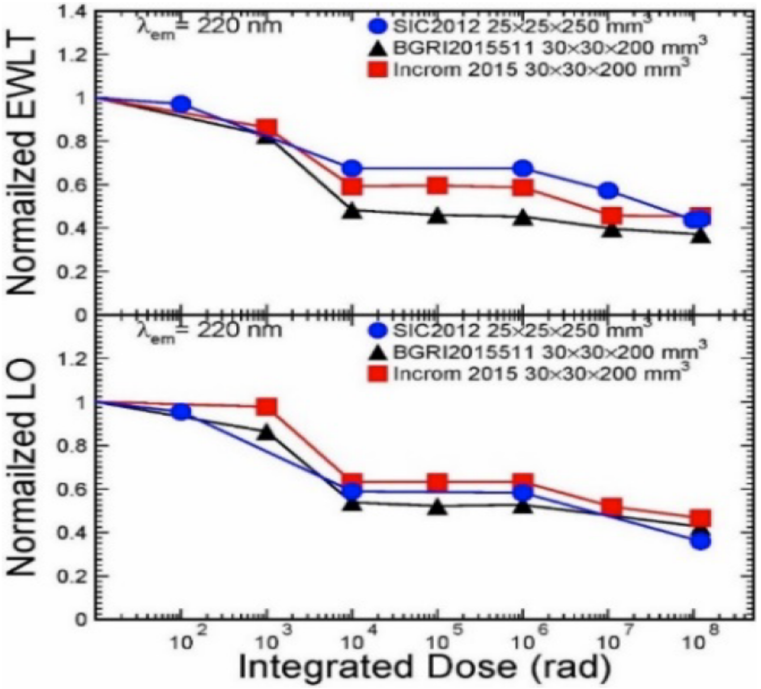

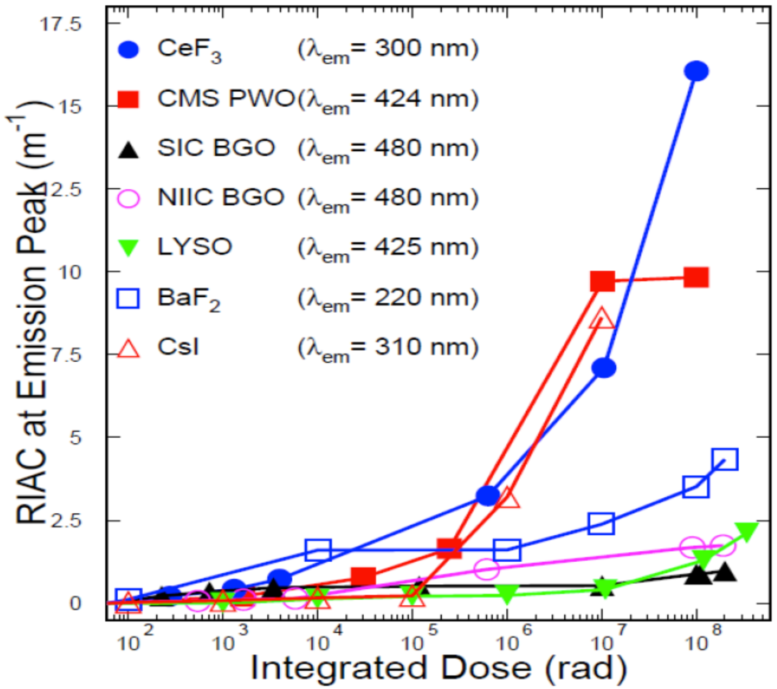

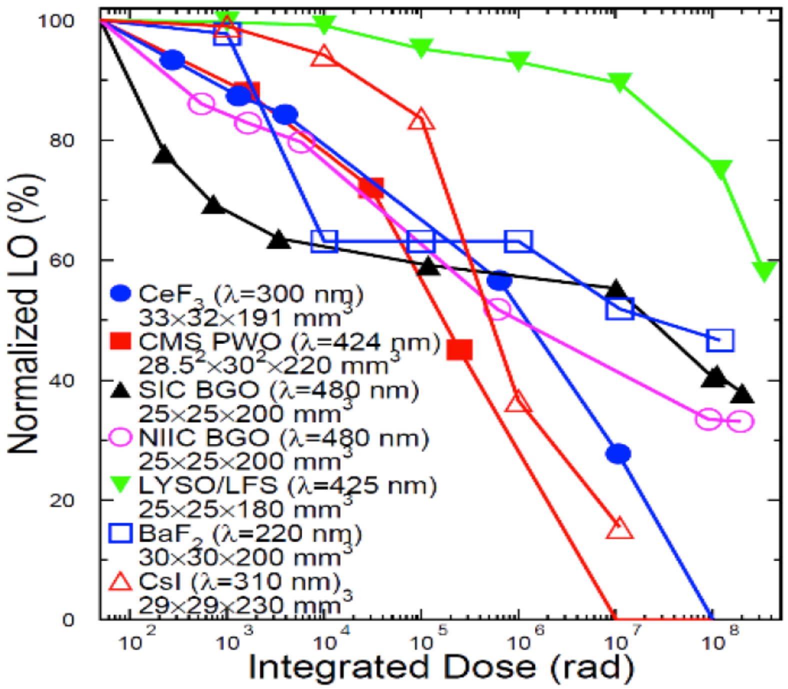

BaF_2:Y for Ultrafast Calorimetry

Increased F/T ratio observed in BGRI BaF_2:Y crystals, Proc. SPIE 10392 (2017)

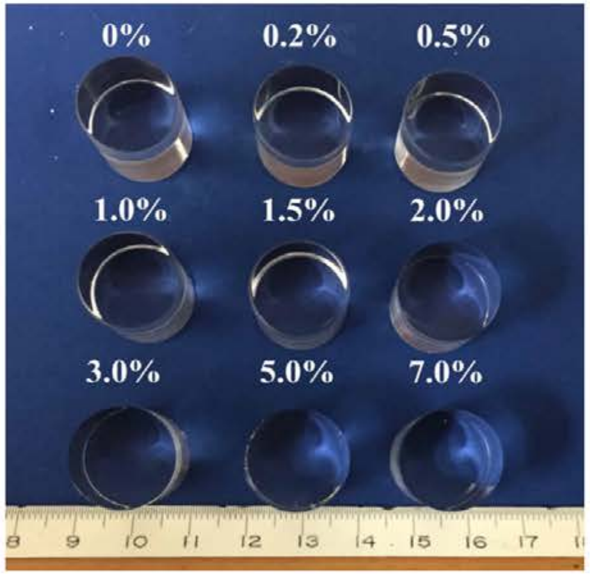

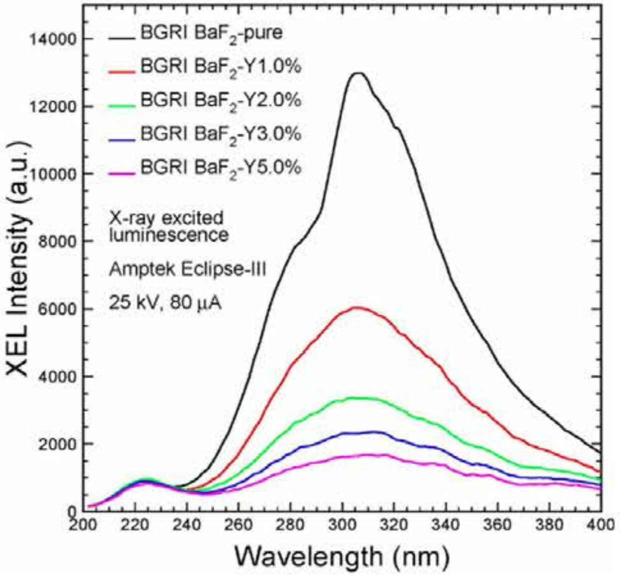

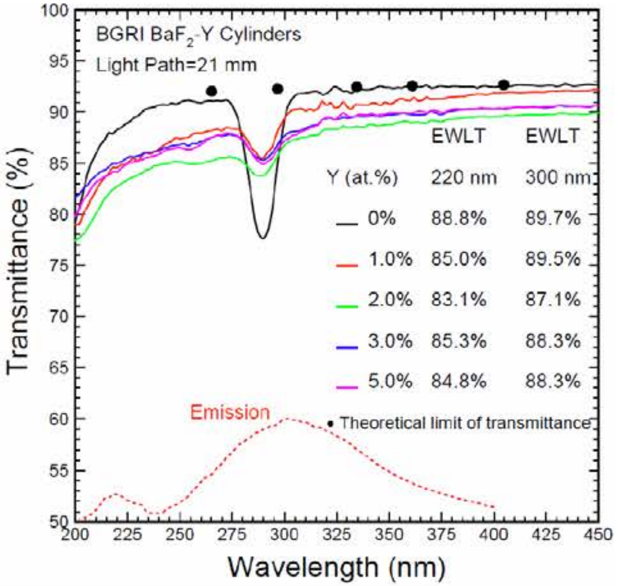

Y (at.%)	EWLT 220 nm	EWLT 300 nm
0%	88.8%	89.7%
1.0%	85.0%	89.5%
2.0%	83.1%	87.1%
3.0%	85.3%	88.3%
5.0%	84.8%	88.3%

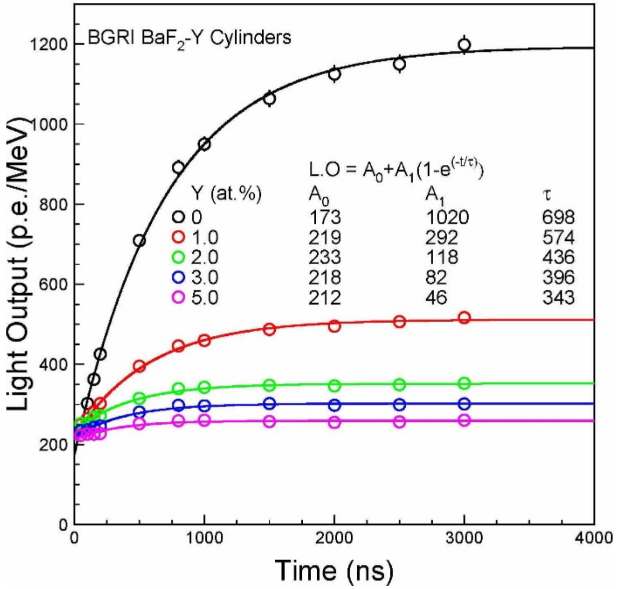

L.O = $A_0+A_1(1-e^{(-t/\tau)})$

Y (at.%)	A_0	A_1	τ
○ 0	173	1020	698
○ 1.0	219	292	574
○ 2.0	233	118	436
○ 3.0	218	82	396
○ 5.0	212	46	343

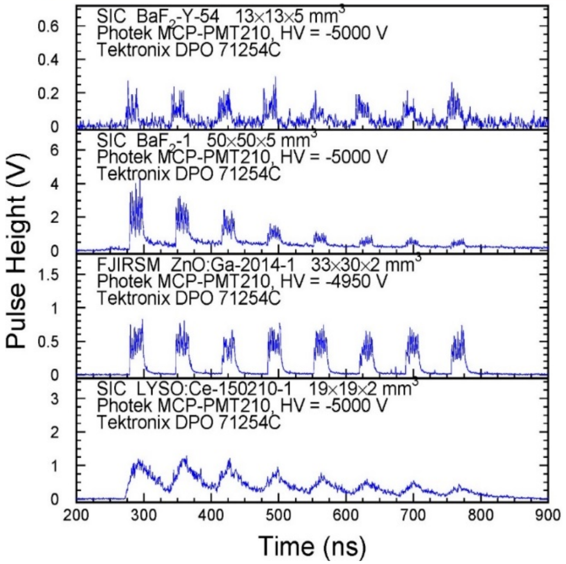

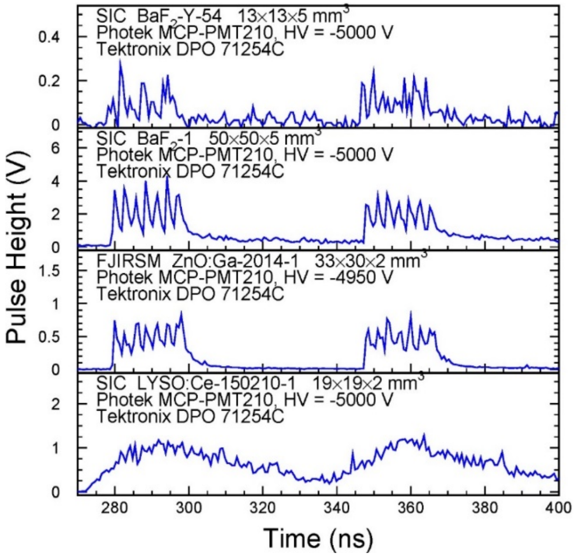

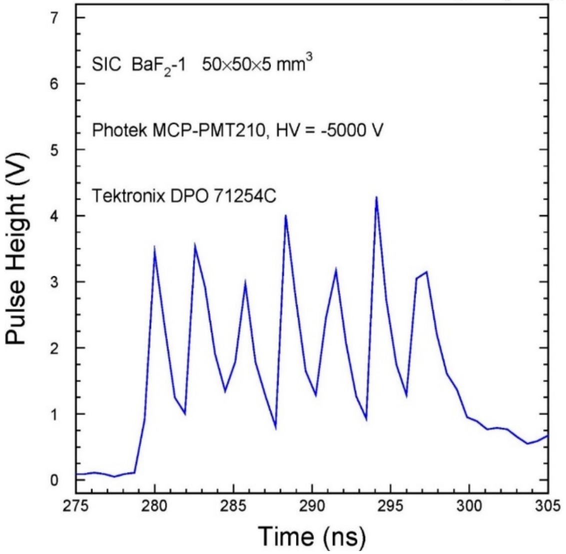

X-ray bunches with 2.83 ns spacing in septuplet are clearly resolved by ultrafast BaF_2:Y and BaF_2 crystals: for GHz Hard X-ray Imaging

NIMA 240 (2019) 223-239

Long BaF_2:Y Crystals for Mu2e-II

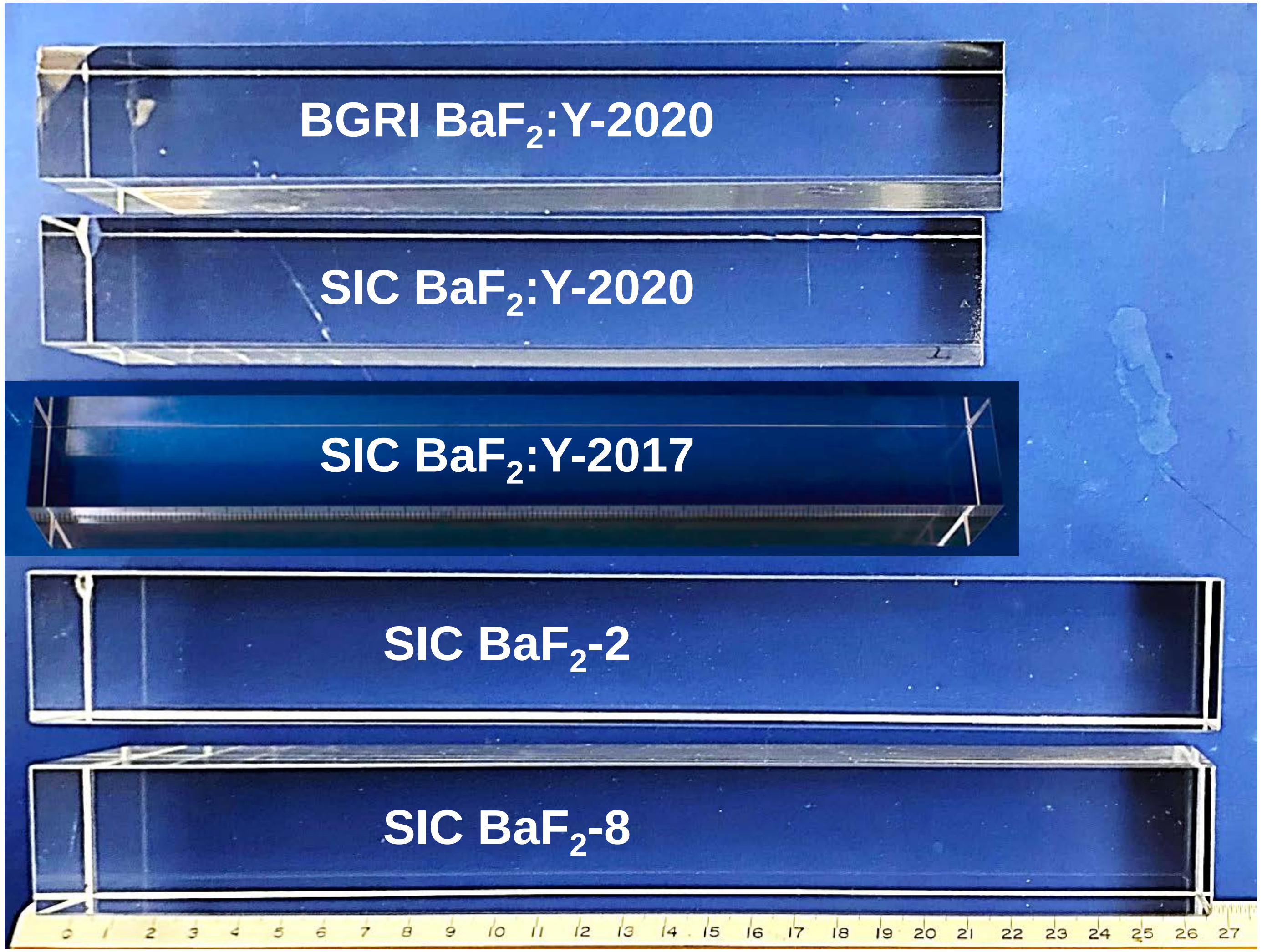

Sample ID	Dimension (mm^3)
BGRI BaF_2:Y-2020	25×25×201
SIC BaF_2:Y-2020	25×25×197
SIC BaF_2:Y-2017	32×32×182
SIC BaF_2-2	30×30×250
SIC BaF_2-8	30×30×250

Gamma-ray Induced Readout Noise RIN:ɣ

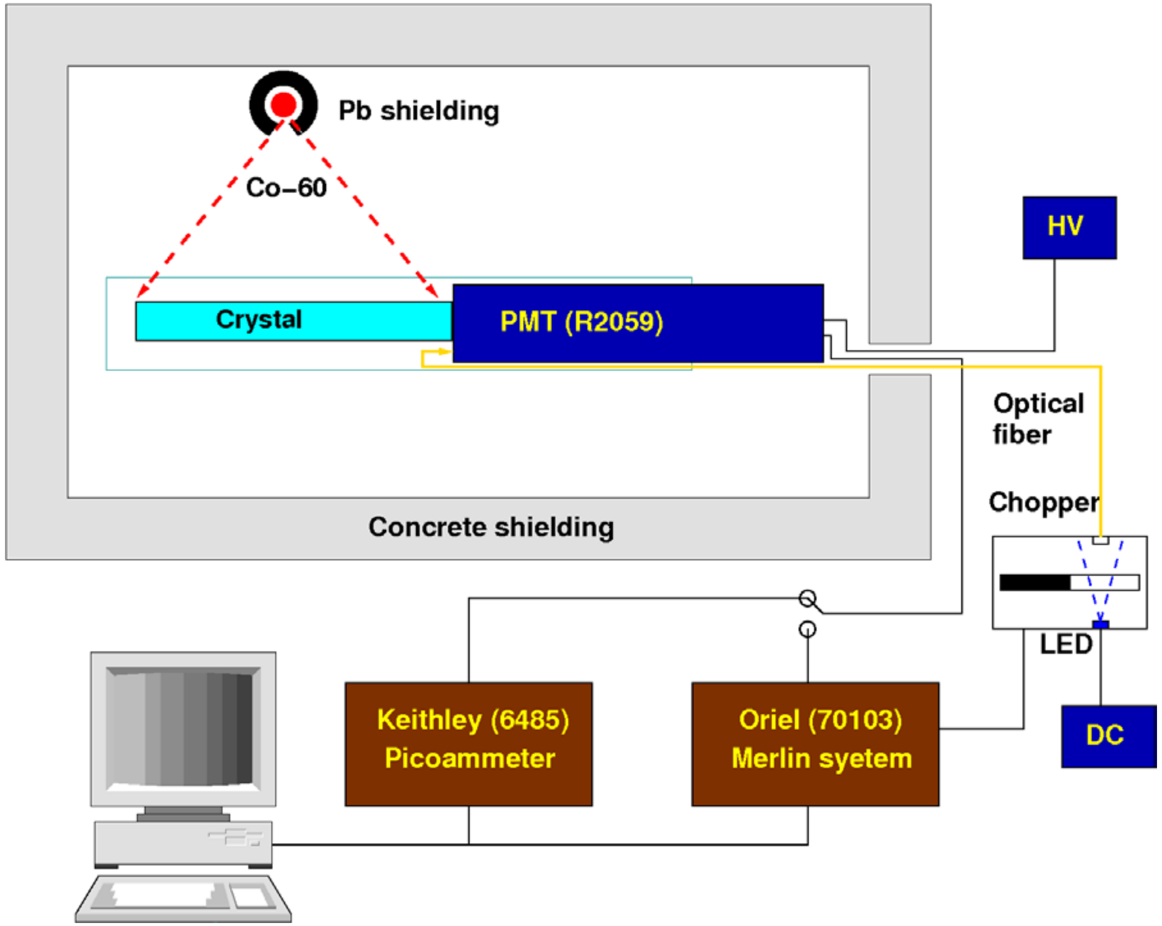

BaF$_2$ crystals, wrapped by Tyvek paper and coupled to the R2059 PMT via an air gap, were irradiated by ^{60}Co ɣ-rays under dose rates of 2 and 23 rad/h

F is defined as the radiation induced photoelectron numbers per second, normalized to the dose rate.
RIN (σ) is defined as the fluctuation of photoelectron number (Q) in the readout gate normalized to the light output (LO) of BaF$_2$

$$F = \frac{\dfrac{Photocurrent}{Charge_{electron} \times Gain_{SiPM}}}{Dose\ rate_{\gamma-ray}\ or\ Flux_{neutron}}$$

$$Q = F \times Dose\ Rate \times Gate\ Length$$

$$\sigma = \frac{\sqrt{Q}}{LO} \quad \text{(MeV)}$$

QE/PDE of four VUV Photodetectors

QE/PDE of four VUV photodetectors for BaF_2 and BaF_2:Y

Paper N05-03 in the virtual IEEE NSS/MIC 2020 Conference Record (2020)

Photodetector	$EWQE/PDE_{fast}$ (%)	$EWQE/PDE_{slow}$ (%)	$EWQE/PDE_{BaF}$ (%)	$EWQE/PDE_{BaF:Y}$ (%)	Relative LO (50 ns)	Relative F_{BaF}	Relative $F_{BaF:Y}$
Hamamatsu R2059	15.2	20.9	20.0	18.7	1.00	1.00	1.00
Photek Solar-Blind	25.6	10.6	13.0	16.1	1.68	0.65	0.86
FBK SiPM w/UV Filter-I	17.8	12.7	13.5	14.7	1.17	0.68	0.79
Hamamatsu MPPC	10.5	9.8	9.9	10.2	0.69	0.50	0.55

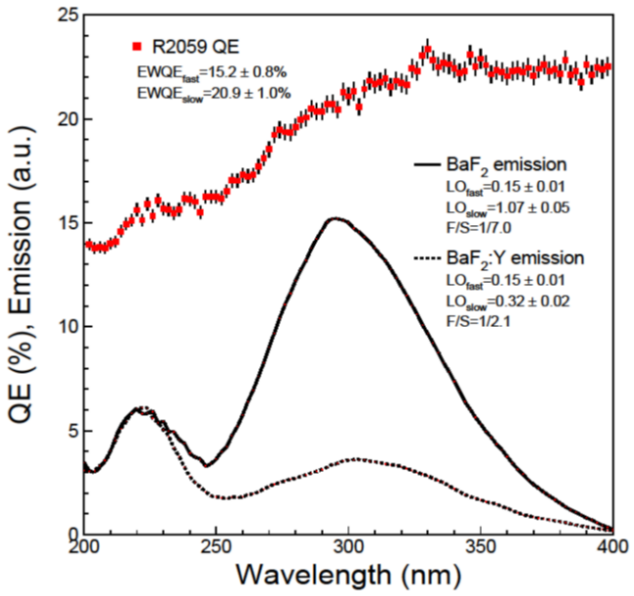

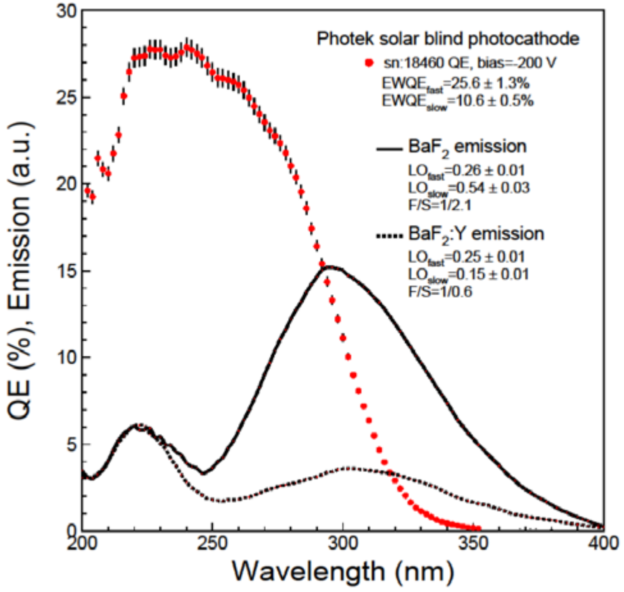

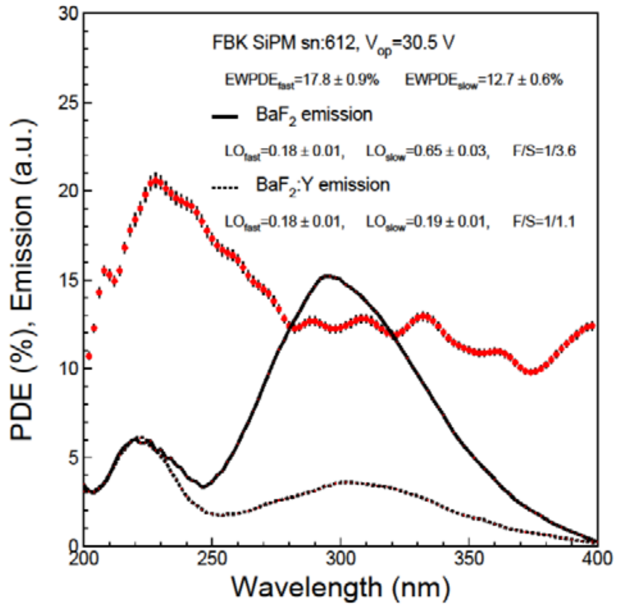

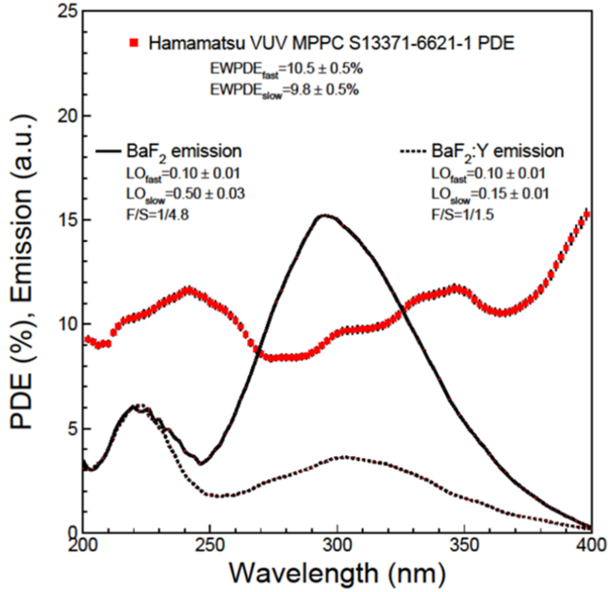

RIN:ɣ for four VUV Photodetectors

Photodetector	EWQE/PDE$_{fast}$ (%)	EWQE/PDE (%)	LO(50 ns) p.e./MeV	F	RIN:ɣ (keV)
BGRI BaF$_2$:Y-2020					
Hamamatsu R2059 PMT	15.2	18.7	53	3.1×10^9	1050
Photek PMT Solar Blind	25.6	16.1	89	2.7×10^9	**580**
FBK SiPM w/UV Filter-I	17.8	14.7	62	2.4×10^9	800
Hamamatsu VUV MPPC	10.5	10.2	37	1.7×10^9	1120
SIC BaF$_2$:Y-2020					
Hamamatsu R2059 PMT	15.2	18.7	45	1.3×10^9	810
Photek PMT Solar Blind	25.6	16.1	76	1.1×10^9	450
FBK SiPM w/UV Filter-I	17.8	14.7	53	1.0×10^9	610
Hamamatsu VUV MPPC	10.5	10.2	31	7.1×10^8	870
BGRI BaF$_2$-1507					
Hamamatsu R2059 PMT	15.2	20.0	46	5.8×10^9	1650
Photek PMT Solar Blind	25.6	13.0	77	3.8×10^9	790
FBK SiPM w/UV Filter-I	17.8	13.5	54	3.9×10^9	1160
Hamamatsu VUV MPPC	10.5	9.9	32	2.9×10^9	1680
SIC BaF$_2$-2					
Hamamatsu R2059 PMT	15.2	20.0	48	5.8×10^9	1590
Photek PMT Solar Blind	25.6	13.0	81	3.8×10^9	760
FBK SiPM w/UV Filter-I	17.8	13.5	56	3.9×10^9	1120
Hamamatsu VUV MPPC	10.5	9.9	33	2.9×10^9	1620

RIN:ɣ is dominated by the slow light, so is reduced by yttrium doping
Solar blind photo-detector reduces RIN:ɣ to less than 0.6 MeV

1 Mrad Damage in Long BaF_2:Y

SIC 2017 BaF_2:Y sample approaches performance of BaF_2 crystals
Recovery is very small for the fast scintillation component

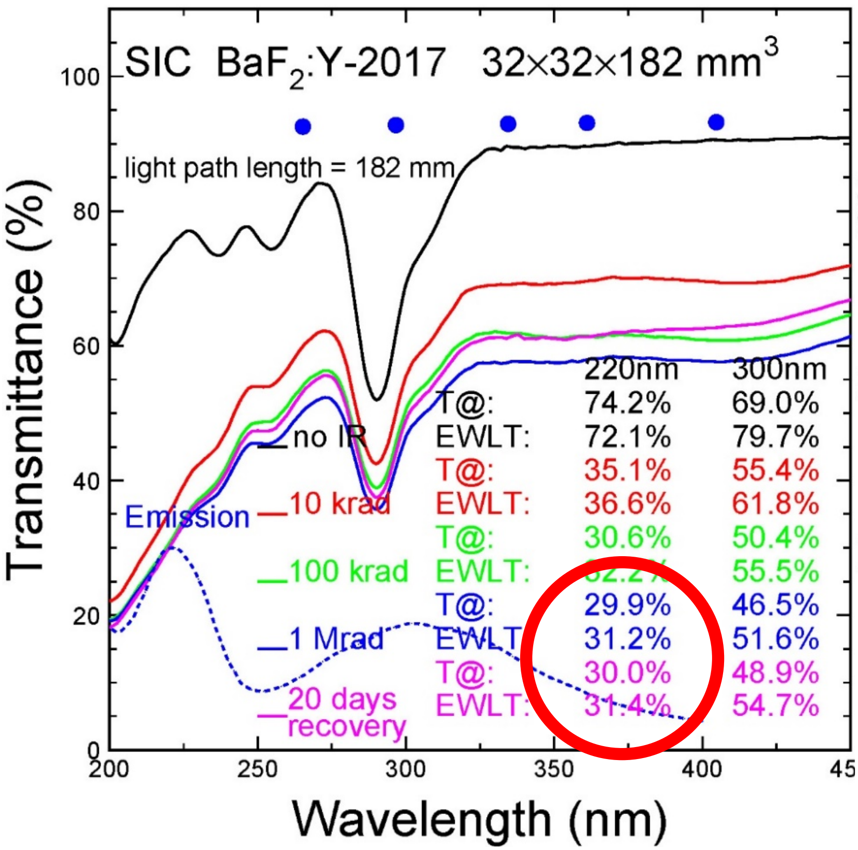

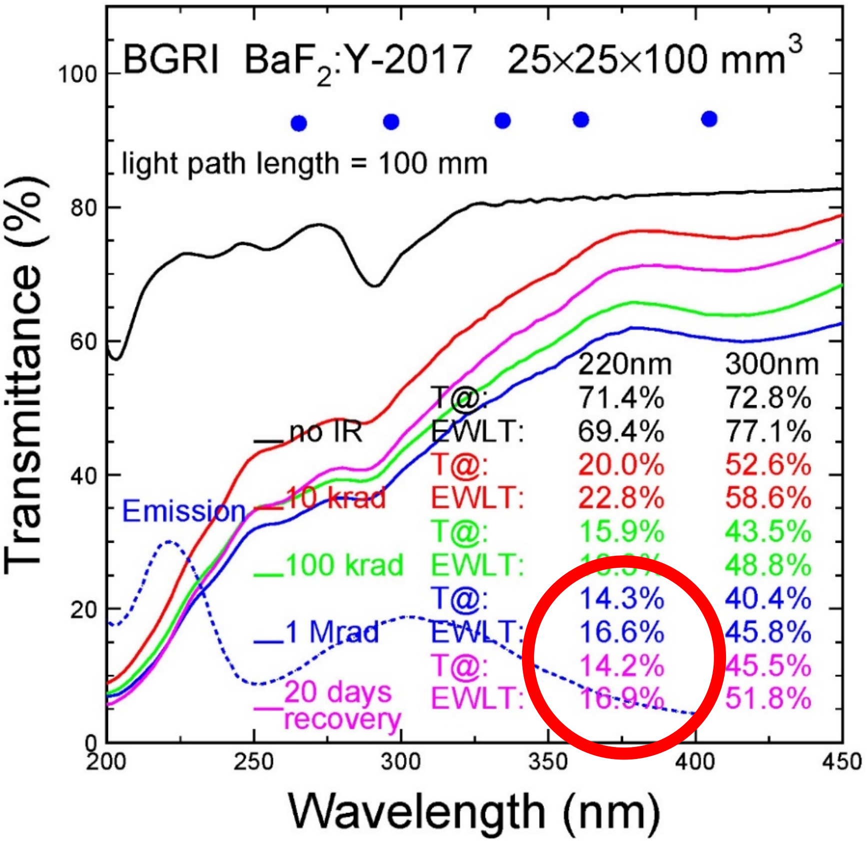

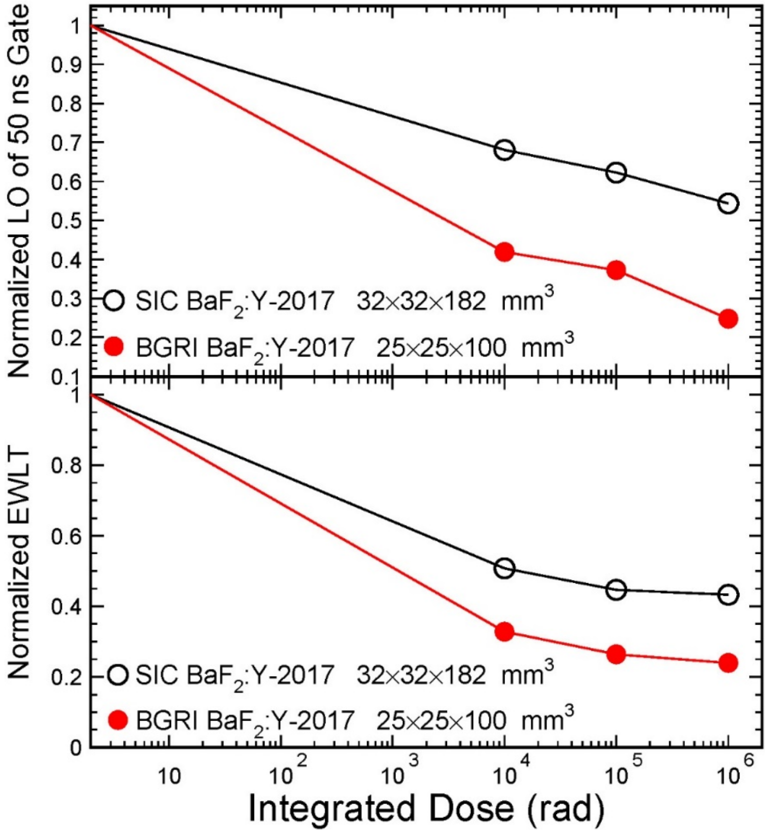

Diverse crystal quality at this stage. R&D needed for improvement

Calvision: Longitudinally Segmented Crystal CAL

Aiming at excellent EM and jet resolutions for Higgs Factory

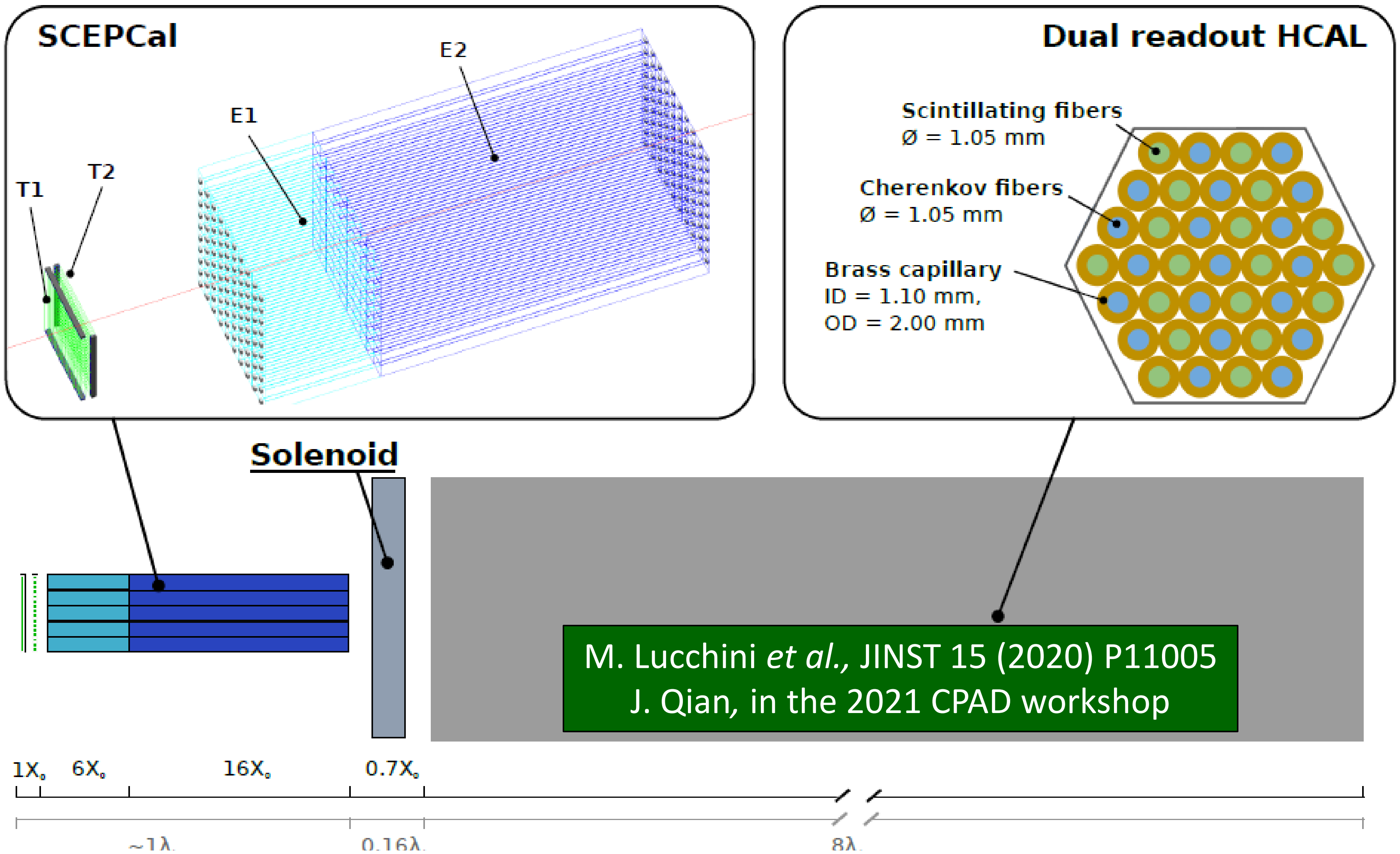

M. Lucchini *et al.*, JINST 15 (2020) P11005
J. Qian, in the 2021 CPAD workshop

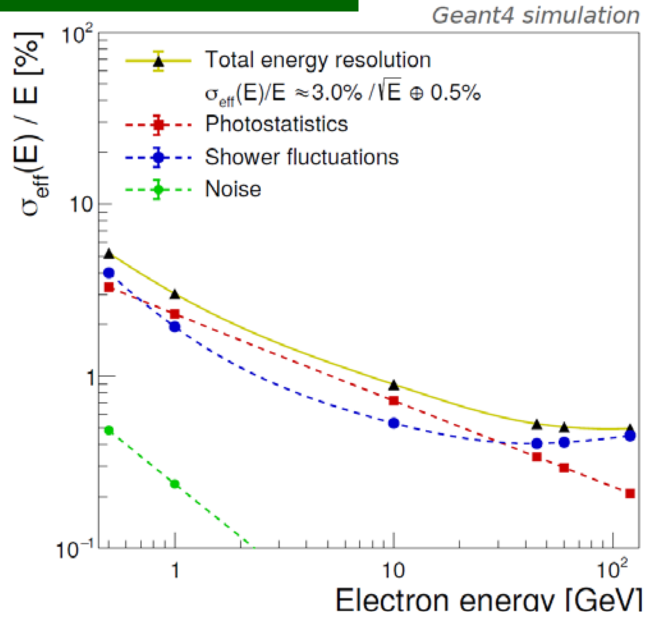

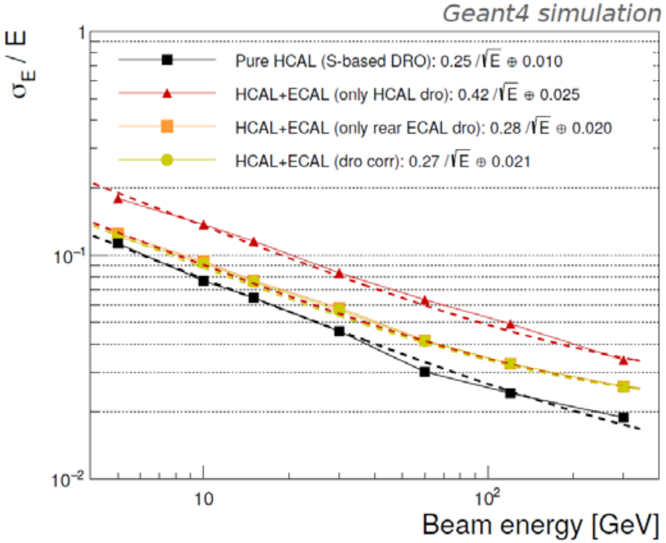

The HHCAL Concept

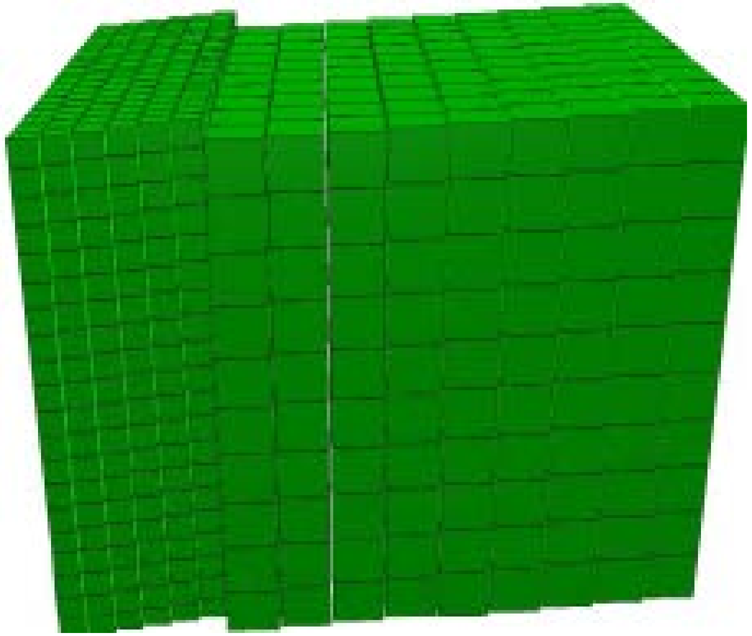

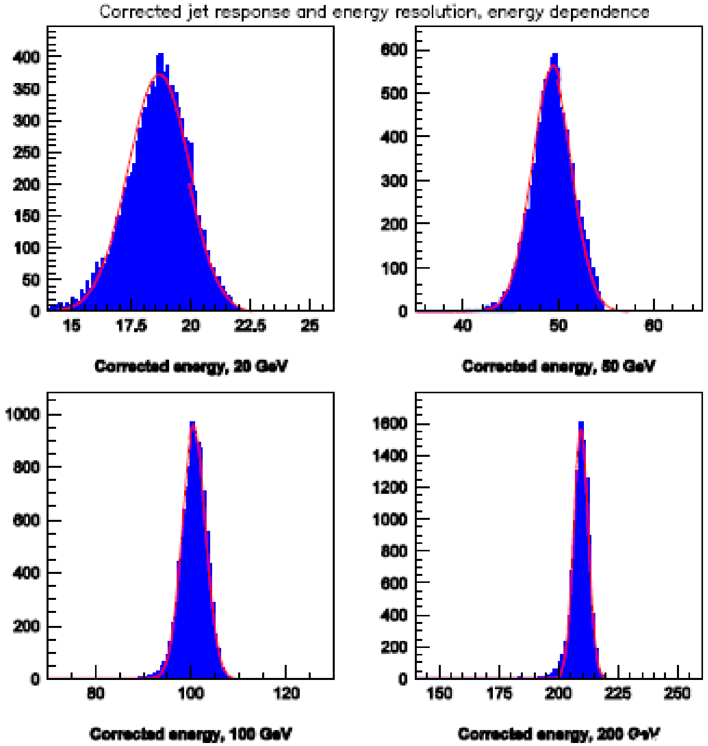

A. Para, H. Wenzel, and S. McGill in Callor2012 Proceedings and A. Benaglia *et al*., IEEE TNS **63** (2016) 574-579: a jet energy resolution at a level of 20%/√E by HHCAL with dual readout of S/C or dual gate.
M. Demarteau, 2021 CPAD Workshop

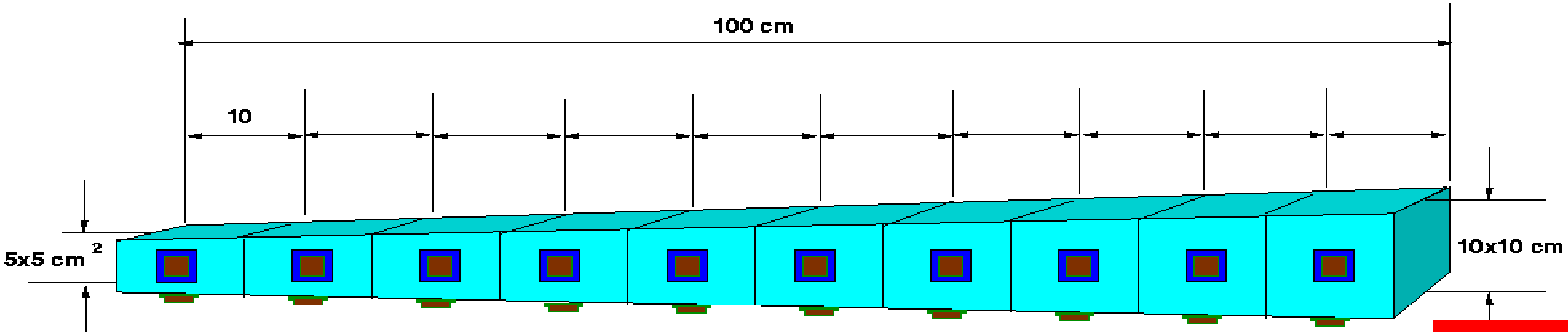

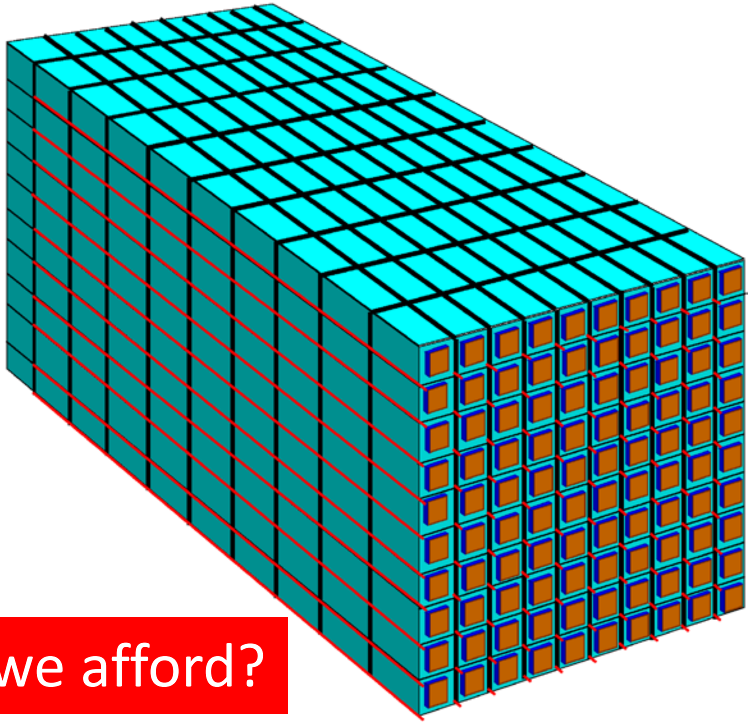

R.-Y. Zhu, ILCWS-8, Chicago: a HHCAL cell with pointing geometry

Can we afford?

Inorganic Scintillators for HHCAL

	BGO	BSO	PWO	PbF_2	PbFCl	Sapphire:Ti	AFO Glass	BaO·2SiO$_2$ Glass[1]	HFG Glass[2]
Density (g/cm^3)	7.13	6.8	8.3	7.77	7.11	3.98	4.6	3.8	5.95
Melting point (℃)	1050	1030	1123	824	608	2040	980[3]	1420[4]	570
X_0 (cm)	1.12	1.15	0.89	0.94	1.05	7.02	2.96	3.36	1.74
R_M (cm)	2.23	2.33	2.00	2.18	2.33	2.88	2.89	3.52	2.45
λ_I (cm)	22.7	23.4	20.7	22.4	24.3	24.2	26.4	32.8	23.2
Z_{eff} value	72.9	75.3	74.5	77.4	75.8	11.2	42.8	44.4	56.9
dE/dX (MeV/cm)	8.99	8.59	10.1	9.42	8.68	6.75	6.84	5.56	8.24
Emission Peak[a] (nm)	480	470	425 420	\	420	300 750	365	425	325
Refractive Index[b]	2.15	2.68	2.20	1.82	2.15	1.76	\	\	1.50
Relative Light Output by PMT[a,c]	100	20	1.6 0.4	\	2.0	0.2 0.9	2.6	5.0 4.0	3.3 6.1
LY (ph/MeV)[d]	35,000	1,500	130	\	150	7,900	450	3,150	150
Decay Time[a] (ns)	300	100	30 10	\	3	300 3200	40	180 30	25 8
d(LY)/dT (%/°C)[d]	-0.9	?	-2.5	\	?	?	?	-0.04	-0.37
Cost ($/cc)	6.0	7.0	7.5	6.0	?	0.6	?	?	?

Low density crystals/glasses

a. Top line: slow component, bottom line: fast component.
b. At the wavelength of the emission maximum.
c. Relative light yield normalized to the light yield of BGO
d. At room temperature (20°C) with PMT QE taken out.

Cost of Mass Produced Crystals (Mar 2019)

Cost effectiveness scaled to X_0: PWO, BGO, CsI, BSO, BaF_2:Y, LYSO

Item	Size (R_MxR_Mx25 X_0)	1 m^3	10 m^3	100 m^3	Scaled to X_0
BGO	22.3×22.3×280 mm	\$8/cc	\$7/cc	\$6/cc	1.23
BaF_2:Y	31.0×31.0×507.5 cm	\$12/cc	\$11/cc	\$10/cc	2.28
LYSO:Ce	20.7x20.7x285 mm	\$36/cc	\$34/cc	\$32/cc	1.28
PWO	20x20x223 mm	\$9/cc	\$8/cc	\$7.5/cc	1.00
BSO	22x22x274 mm	\$8.5/cc	\$7.5/cc	\$7.0/cc	1.29
CsI	35.7x35.7x465 mm	\$4.6/cc	\$4.3/cc	\$4.0/cc	2.09

Summary

- The HL-LHC and FCC-hh requires fast and rad hard calorimetry. The **RADiCAL** concept uses radiation hard LuAG:Ce ceramics as WLS for LYSO:Ce crystals for an ultra-compact, fast and longitudinally segmented shashlik calorimeter. R&D is needed for LuAG:Ce WLS.
- Undoped BaF_2 crystals provide ultrafast light with sub-ns decay time and a good radiation hardness up to 100 Mrad. Yttrium doping suppresses its slow light and promises a **ultrafast calorimeter**. R&D is needed for optimizing yttrium doping and radiation hardness in large size BaF_2:Y crystals for Mu2e-II. Solar-blind VUV photodetectors are also needed for controlling the radiation induced readout noise.
- The longitudinally segmented **Calvision** crystal ECAL with dual readout combined with a Dream HCAL promises excellent EM and HAD resolutions for the Higgs factory.
- Homogeneous HCAL (**HHCAL**) promises the best jet mass resolution by total absorption with a challenge in cost. R&D is needed for cost-effective mass produced inorganic scintillators.

Acknowledgements: DOE HEP Award DE-SC0011925

Cost-Effective Sapphire Crystals for HHCAL

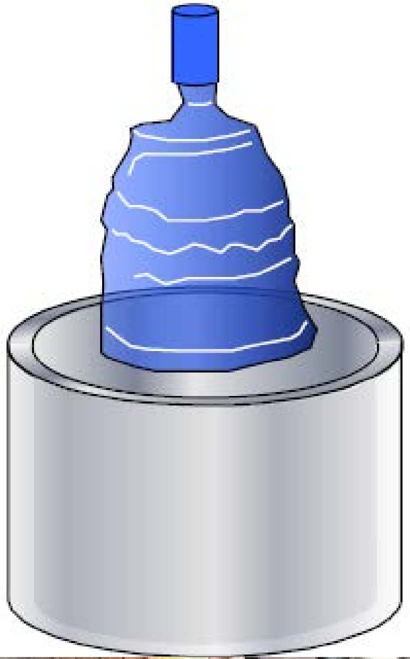

Prof. Xu Jun of Tongji University: Sapphire crystals by Kyropoulos (KY) technology
A producer can grow 1,000 tons ingots annually with 400 to 450 kg/ingot
Cost of mass-produced Sapphire crystals including processing: less than $1/cc

Sapphire Crystal	Weight (g)	Size (cm)	Unit Price	Comment
Ingot Boule	400,000	Φ50×55	US$12,000/pc	Undoped
Cutting/Polishing	4	1×1×1	**~US$0.6/cc**	Undoped

Sapphire:Ti Emission and Transmittance

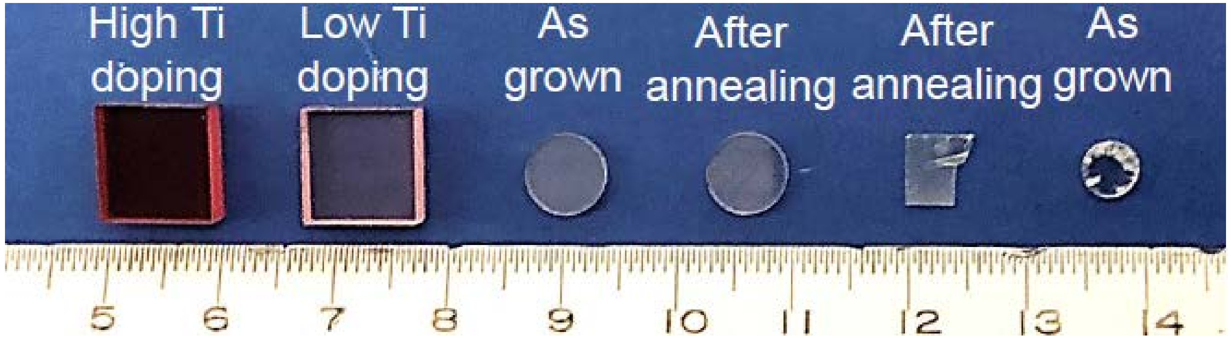

ID	Dimension (mm³)	#	Polishing
Al_2O_3:Ti-1,2	**10×10×4**	**2**	**Two faces**
Al_2O_3:C-1,2	Φ7×1	2	Two faces
Lu_2O_3:Yb	6.4×4.8×0.4	1	Two faces
$LuScO_3$:Yb	Φ4.8×1.3	1	Two faces
All samples received on April 15st 2019 (Monday)			

A weak emission at 325 nm with 150 ns decay time
A strong emission at 755 nm with 3 μs decay time

Fast @325 nm

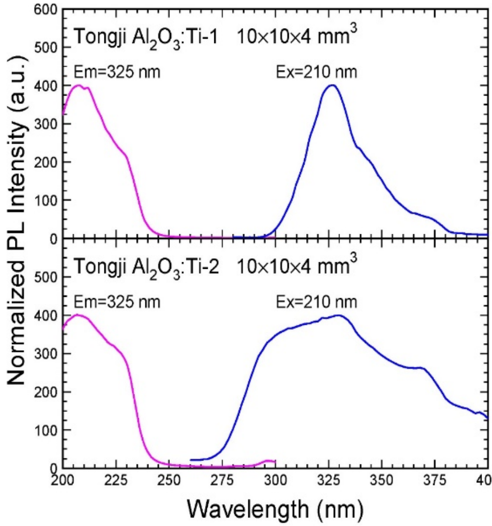

Slow @ 755 nm

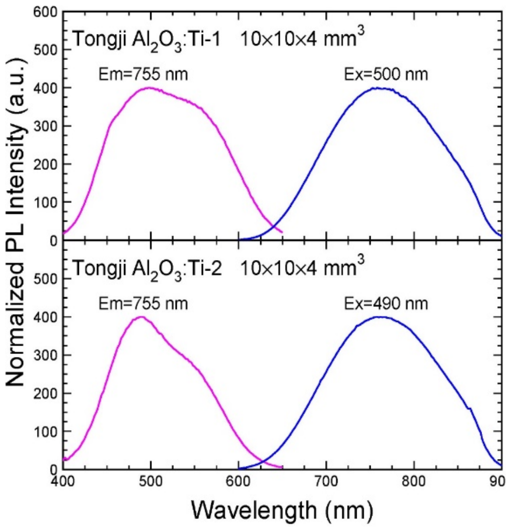

EWLT for Fast & Slow

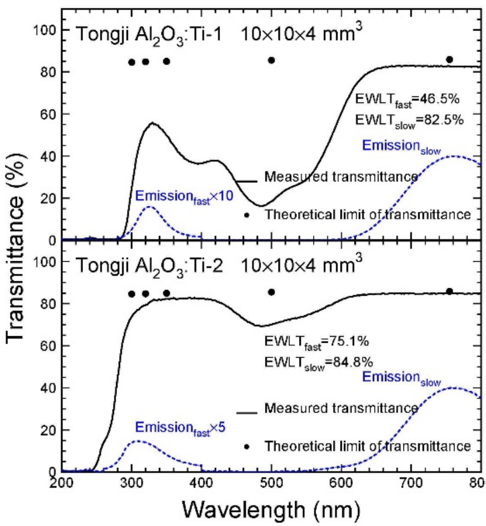

Fast Decay: 162 ns

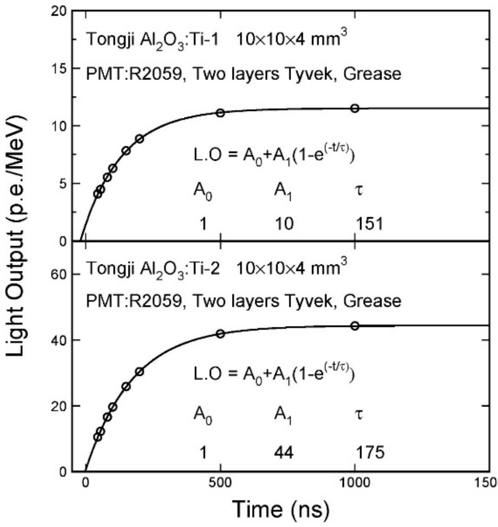

Slow Decay: 3.2 μs

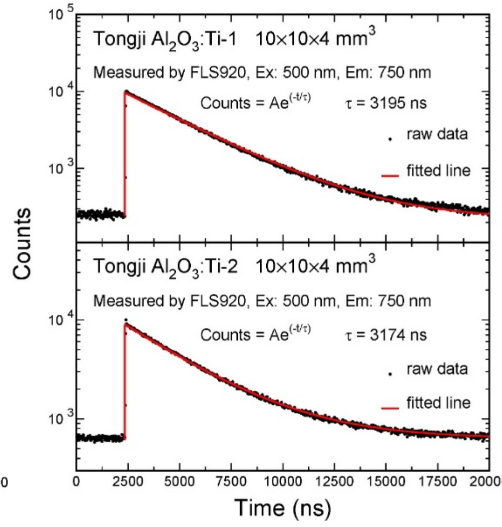

Light Output for Al_2O_3:Ti-1 and 2

Fast/slow component: 0.3k/6.4k and 1.3k/6.6k photons/MeV
Total: 6.7k and 7.9k photons/MeV, compatible with BGO

PHS: Al_2O_3:Ti-1/2

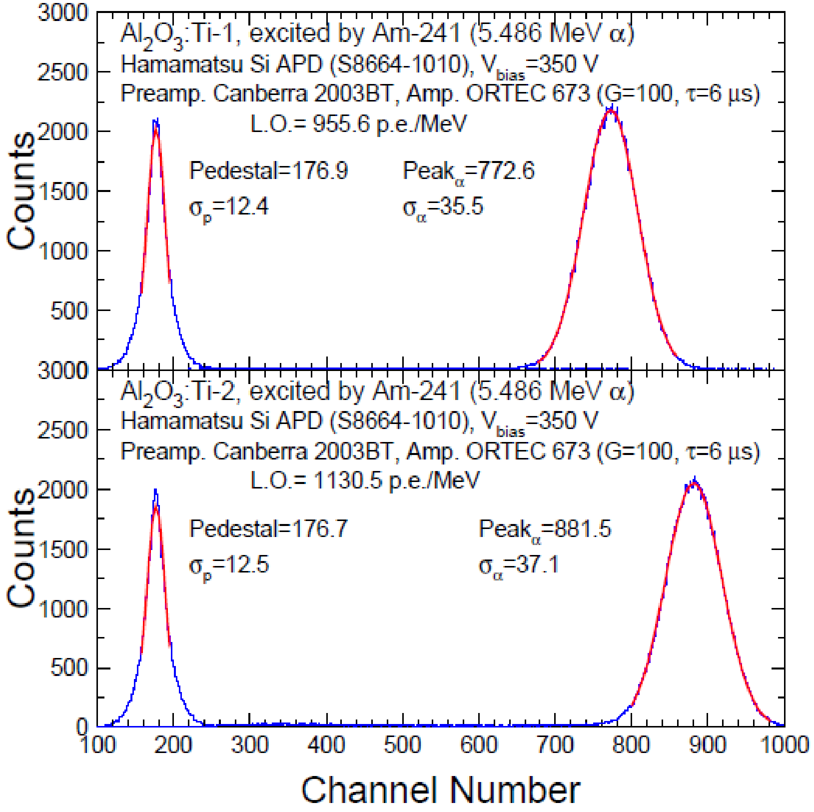

R2059 EWQE

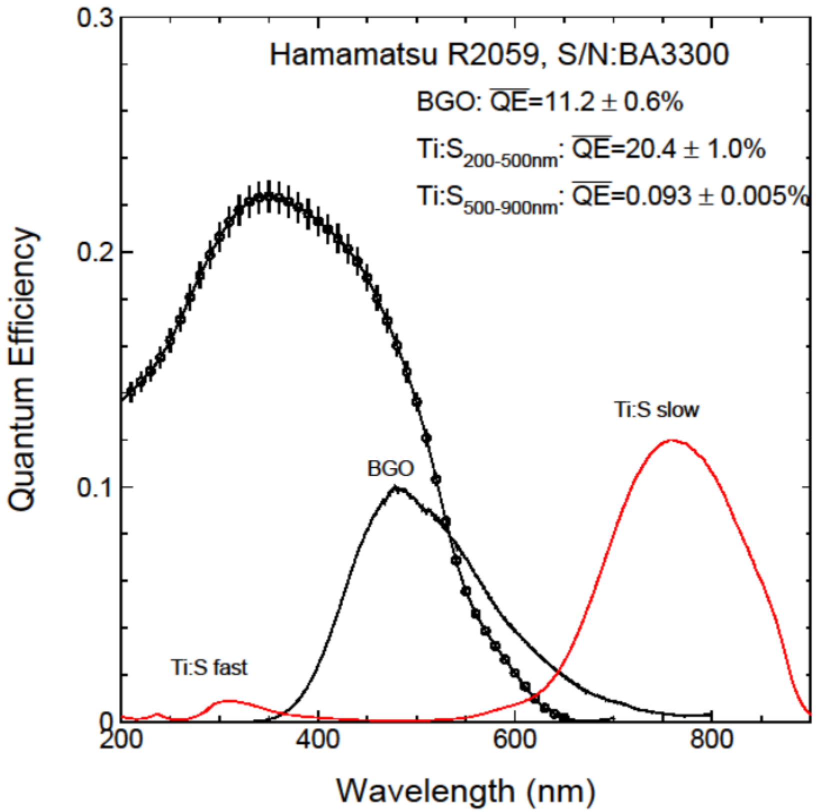

S6654-1010 EWQE